

REPORT DOCUMENTATION PAGE				Form Approved OMB No. 0704-0188	
Public reporting burden for this collection of information is estimated to average 1 hour per response, including the time for reviewing instructions, searching existing data sources, gathering and maintaining the data needed, and completing and reviewing the collection of information. Send comments regarding this burden estimate or any other aspect of this collection of information, including suggestions for reducing the burden, to Department of Defense, Washington Headquarters Services, Directorate for Information Operations and Reports (0704-0188), 1215 Jefferson Davis Highway, Suite 1204, Arlington, VA 22202-4302. Respondents should be aware that notwithstanding any other provision of law, no person shall be subject to any penalty for failing to comply with a collection of information if it does not display a currently valid OMB control number. PLEASE DO NOT RETURN YOUR FORM TO THE ABOVE ADDRESS.					
1. REPORT DATE (DD-MM-YYYY) 13-02-2006		2. REPORT TYPE Final Report		3. DATES COVERED (From – To) 1 October 2003 - 01-Oct-05	
4. TITLE AND SUBTITLE Tm Doped Fiber Laser Pumped by a Cladding-Pumtped Er,Yb Fiber Laser			5a. CONTRACT NUMBER FA8655-03-1-3057		
			5b. GRANT NUMBER		
			5c. PROGRAM ELEMENT NUMBER		
6. AUTHOR(S) Dr. William A Clarkson			5d. PROJECT NUMBER		
			5d. TASK NUMBER		
			5e. WORK UNIT NUMBER		
7. PERFORMING ORGANIZATION NAME(S) AND ADDRESS(ES) University of Southampton Southampton SO17 1BJ United Kingdom				8. PERFORMING ORGANIZATION REPORT NUMBER N/A	
9. SPONSORING/MONITORING AGENCY NAME(S) AND ADDRESS(ES) EOARD PSC 821 BOX 14 FPO 09421-0014				10. SPONSOR/MONITOR'S ACRONYM(S)	
				11. SPONSOR/MONITOR'S REPORT NUMBER(S) Grant 03-3057	
12. DISTRIBUTION/AVAILABILITY STATEMENT Approved for public release; distribution is unlimited.					
13. SUPPLEMENTARY NOTES					
14. ABSTRACT This report results from a contract tasking University of Southampton as follows: The Grantee will investigate a) optimization of the cladding-pumped Er-Yb doped fiber laser (EYDFL) for efficient pumping of Tm-doped fibers. b) Investigation of core-pumping of Tm-doped fibers using the EYDFL developed in task a, c) design, fabrication and demonstration of a high-power, core-pumped, multimode Tm-doped fiber laser, and d) demonstration of high-power, single-mode output from the core-pumped Tm-doped fiber laser.					
15. SUBJECT TERMS EOARD, lasers and laser engineering, Laser amplifiers, Fibre Lasers, infrared technology					
16. SECURITY CLASSIFICATION OF:			17. LIMITATION OF ABSTRACT UL	18, NUMBER OF PAGES 46	19a. NAME OF RESPONSIBLE PERSON DONALD J SMITH
a. REPORT UNCLAS	b. ABSTRACT UNCLAS	c. THIS PAGE UNCLAS			19b. TELEPHONE NUMBER (Include area code) +44 (0)20 7514 4953

EOARD Project

Contract order number: FA8655-03-1-3057

Tm doped fiber laser pumped by a cladding-pumped Er,Yb fiber laser

Final Report

W. A. Clarkson, D.Y. Shen, P. J. Jander and J. K. Sahu

Optoelectronics Research Centre
University of Southampton
Southampton, SO17 1BJ
United Kingdom

Contents:

1.0 Introduction

2.0 Objectives

3.0 Development of high-power Er,Yb-doped fiber pump sources

3.1 Introduction

3.2 Diode-stack pump module and coupling scheme

3.3 Er,Yb fiber laser design

3.4 Laser performance

3.5 Tunable Er,Yb fiber laser

3.6 Thermally-induced damage and its mitigation

3.7 Prospects for further power scaling

4.0 Tm fiber source

4.1 Introduction

4.2 Tm fiber designs

4.3 Pumping geometries – Cladding versus core pumping

4.4 Cladding-pumped Tm fiber lasers (1550nm versus 800nm)

4.5 Core-pumped Tm fiber laser

4.6 Q-switched operation of a Tm fiber laser

4.7 Summary and future prospects

5.0 Conclusions and future work

6.0 References

7.0 Publications

Appendices:

- A1 Highly efficient Er,Yb-doped fiber laser with 188W free-running and >100W tunable output power.
- A2 High-power widely tunable Tm fiber lasers in cladding-pumped and core-pumped cavity configurations

1.0 INTRODUCTION

High power solid-state lasers operating in the two-micron spectral regime have numerous applications and, in addition, provide an excellent starting point for nonlinear frequency conversion to the mid-infrared ($\sim 3\text{-}5\mu\text{m}$) spectral region. The conventional way to achieve laser output in the $\sim 2\mu\text{m}$ regime is via diode pumping of crystals doped with Tm or doped with Tm and Ho. However, the combination of a low emission cross-section and the quasi-three-level nature, which are typical of the laser transitions involved, leads to a requirement for high pumping intensities, which lead, in turn, to high thermal loading densities and strong thermal effects. The latter can be highly detrimental to laser performance, particularly in laser configurations (e.g. end-pumped lasers) in which the pump light is deposited in a highly non-uniform manner, owing to the very strong and highly aberrated thermal lensing that results. As a consequence, power-scaling whilst maintaining diffraction-limited (TEM_{00}) beam quality and high efficiency is extremely difficult.

Cladding-pumped Tm-doped silica fiber lasers offer an alternative route to high output power in the two-micron spectral region. The main attractions of cladding-pumped fiber sources compared to conventional ‘bulk’ solid-state lasers are derived directly from the geometry, which allows simple thermal management with waste heat distributed over a long length of fiber reducing the likelihood of damage due to melting or fracture. Furthermore, the wave guiding properties of the core can be easily tailored to select a single-spatial-mode output beam with relative immunity from the problem of thermal lensing. Prior to this project commencing, cladding-pumping of Tm-doped silica fiber lasers by 785-795nm diode lasers had already yielded output powers up to 14W (limited by available pump power) [1], and wavelength tunable operation from 1860-2090nm at multi-watt power levels [2]. Further increase in output power, as well as extension of the tuning range to shorter wavelengths would benefit a number of applications. However, this is rather difficult via the $\sim 785\text{-}795\text{nm}$ pumping route for several reasons: Firstly, further power scaling is hindered by the limited availability of commercial high-power diode sources (e.g. diode-stacks) at the required operating wavelengths, and by the low Stokes efficiency (and hence high fractional heating). Secondly, extending the tuning range to shorter wavelengths is rather difficult because of the high re-absorption loss at shorter wavelengths. The situation is further exacerbated in a cladding-pumped fiber laser because of the need to use a relatively long length of fiber for efficient pump absorption. This problem arises as a direct result of the low brightness from high-power diode pump sources.

The main aim of this research program was to explore a simple alternative approach for power scaling of Tm-doped fiber lasers and at the same time extending the wavelength tuning range to much shorter wavelengths. Our approach is based on a hybrid fiber laser scheme, where a cladding-pumped Er,Yb fiber laser operating in the $1.56\text{-}1.62\mu\text{m}$ spectral region is used to pump ‘in-band’ a Tm-doped silica fiber laser. The main goal of the project was to demonstrate efficient, high-power ($>10\text{W}$) operation of a Tm-doped fiber laser with operating wavelength tunable over a very wide range ($\sim 1730\text{nm}$ to $\sim 2060\text{nm}$), and to show that this approach offers the potential for scaling output power to much higher levels.

2.0 OBJECTIVES

The hybrid fiber laser scheme offers many potential advantages over direct diode-pumping of double-clad Tm-doped fibers. The rationale behind this approach is as follows: Firstly, high-power diode-stacks with operating wavelengths in the 910-980nm band suitable for pumping Er,Yb fiber lasers are commercially available. Thus, cladding-pumping of Er,Yb fiber lasers provides a relatively simple means for generating high power in the 1560-1620nm spectral region in a single-mode or slightly multimode output beam. Secondly, the absorption peak in Tm-doped silica for the $^3\text{H}_6 \rightarrow ^3\text{F}_4$ transition is at 1640 nm and is very broad (~150nm), allowing efficient pumping of a Tm fiber laser by an Er,Yb fiber laser. This approach has the advantage over direct cladding-pumping of Tm fiber lasers with 790nm diodes that the effective pump absorption length in a core-pumped or a small cladding-to-core area ratio cladding-pumped configuration is much shorter for a given Tm concentration, allowing very short devices lengths to be used, and hence offering the prospect of wavelength tunability over a wider fraction of the Tm^{3+} emission spectrum and efficient operation at much shorter wavelengths (down to ~1720nm). Another advantage is that no excited-state absorption occurs at a pumping wavelength ~1.6 μm (which is not the case at pump wavelengths at ~0.79 μm and ~1.06 μm). The overall result is that it should be possible to achieve slope efficiencies with respect to launched power close to the maximum photon conversion efficiency (~80-90% depending on the operating wavelength). Thus, the main theme of this project was to explore this route for simultaneously increasing the output power and extending the range of operating wavelengths of Tm-doped silica fiber lasers, with particular emphasis on short wavelength operation.

The main objectives of the research program were as follows:

- (a) To formulate a strategy for power scaling of cladding-pumped Er,Yb fiber lasers and to develop a high-power Er,Yb fiber with a good beam quality ($M^2 < 2$) for efficient pumping of Tm-doped silica fibers in both core-pumped and cladding-pumped laser configurations.
- (b) To investigate cladding-pumping of Tm fiber lasers by the high power Er,Yb fiber laser developed in stage (a) and to demonstrate an ultra-efficient, high-power Tm fiber laser with output power well in excess of 10W and with a wide wavelength tuning range.
- (c) To investigate core-pumped or (small cladding-to-core area ratio cladding-pumped) Tm fiber laser configurations with the aim of demonstrating a Tm fiber laser with output power >10W and with operating wavelength tunable to short wavelengths (<1750nm).
- (d) To formulate a strategy for further power scaling of Tm fiber lasers.

3.0 DEVELOPMENT OF HIGH-POWER ERBIUM-DOPED FIBER PUMP SOURCES

3.1 Introduction

Cladding-pumped Er-doped fiber lasers offer the prospect of high output power and high

brightness in the $\sim 1.5\text{--}1.6\mu\text{m}$ regime, with relative immunity from the effects of heat generation which are often so detrimental to conventional bulk lasers. Another attractive feature of fiber lasers is wavelength flexibility. The broad transition linewidths that are typical in glass hosts allows fiber laser wavelengths to be tuned over a wide range. For example, cladding-pumped fiber lasers based on erbium have been demonstrated at multi-watt power levels with wavelength tunable operation covering the wavelength range $\sim 1.53\mu\text{m}$ to $\sim 1.62\mu\text{m}$ [3,4]. The combination of wavelength flexibility, high efficiency and good beam quality makes Er fiber lasers excellent pump sources for bulk Er lasers and Tm fiber lasers. However, scaling the output power of Er-doped fiber lasers in the $1.5\text{--}1.6\mu\text{m}$ regime is more challenging than for Yb-doped fiber lasers operating in the $1\mu\text{m}$ wavelength regime due to the larger quantum defect, which results in higher thermal loading. Moreover, for efficient operation of cladding pumped Er-doped fiber devices it is necessary to co-doped with Yb^{3+} ions to increase the pump absorption coefficient and to broaden the absorption band to $\sim 910\text{--}980\text{nm}$ to better match the emission wavelengths available from high power diode pump sources. A relatively high pump absorption coefficient is necessary to keep the device length short and hence the background loss to an acceptable level in cladding-pumped devices. Sensitization of Er-doped fibers with Yb has become a very well-established technique [5,6]. In this pumping scheme (see Fig.1) the Yb^{3+} ions are excited to the $^2\text{F}_{5/2}$ level and the Er^{3+} ions are then excited by non-radiative energy-transfer from the Yb^{3+} ions followed by rapid relaxation to the upper laser level ($^4\text{I}_{13/2}$). At the time this project commenced the maximum power demonstrated via this pumping scheme from a cladding-pumped Er,Yb fiber laser was 103W from a simple (non-tunable) laser configuration [7]. It was noted that lasing on the Er^{3+} transition at $\sim 1.5\mu\text{m}$ was accompanied by lasing on the Yb^{3+} transition at $\sim 1\mu\text{m}$, thereby reducing the lasing efficiency at $1.5\mu\text{m}$. This problem highlights the need for very careful selection and control of the Er^{3+} and Yb^{3+} ion concentrations to ensure efficient energy-transfer from Yb^{3+} to Er^{3+} and to suppress parasitic lasing on the Yb^{3+} transition at $\sim 1\mu\text{m}$, whilst maintaining flexibility in the choice of operating wavelength.

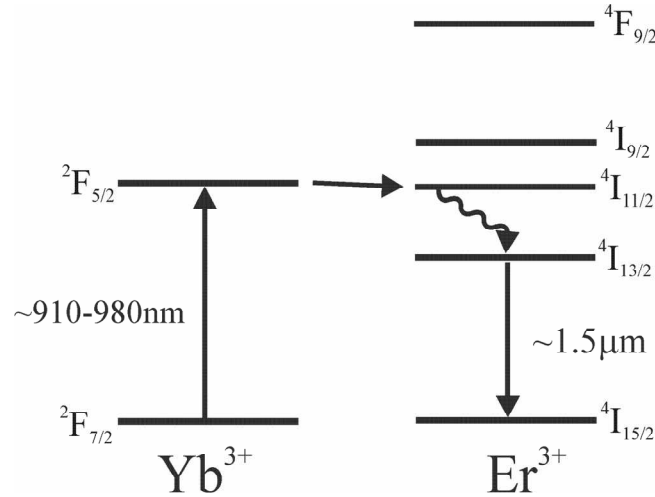


Figure 1: Energy level diagram of Yb and Er ions in silica.

3.2 Diode-stack pump module and coupling scheme

Efficient coupling of high pump power from relatively low brightness diode sources is a very important element of the overall fiber laser design. At present, diode-stacks provide the highest output power of any commercially available diode source and hence are potentially attractive as pump sources for scaling fiber lasers to high power levels. However, the main disadvantage of diode-stacks is the poor quality of their output beams. The beam propagation factor parallel to the diode array, M_x^2 , is typically ~ 1500 - 2000 , and is many times larger than the beam propagation factor, M_y^2 (after fast-axis collimation), in the stacking direction, making it difficult to focus to the small beam sizes required for efficient cladding pumping. For this project, we employed a pump source comprising two 12-bar 500W diode-stacks at 976nm, and a simple a spatial multiplexing and polarization combining scheme to yield a beam which could be launched efficiently into our Er,Yb-doped double-clad fiber (EYDF). The pump combining optics and delivery optics are shown schematically in Fig. 2. The output from each bar on the two stacks was collimated in the fast and slow directions by high numerical aperture fast-axis collimating lenses and slow axis lens arrays respectively. The resulting beams from the two diode-stacks were then combined by inter-leaving using a slotted-mirror beam-combiner to produce a beam with $M_x^2 \approx 400$ and $M_y^2 \approx 150$. The size of the spatially-combined beam after

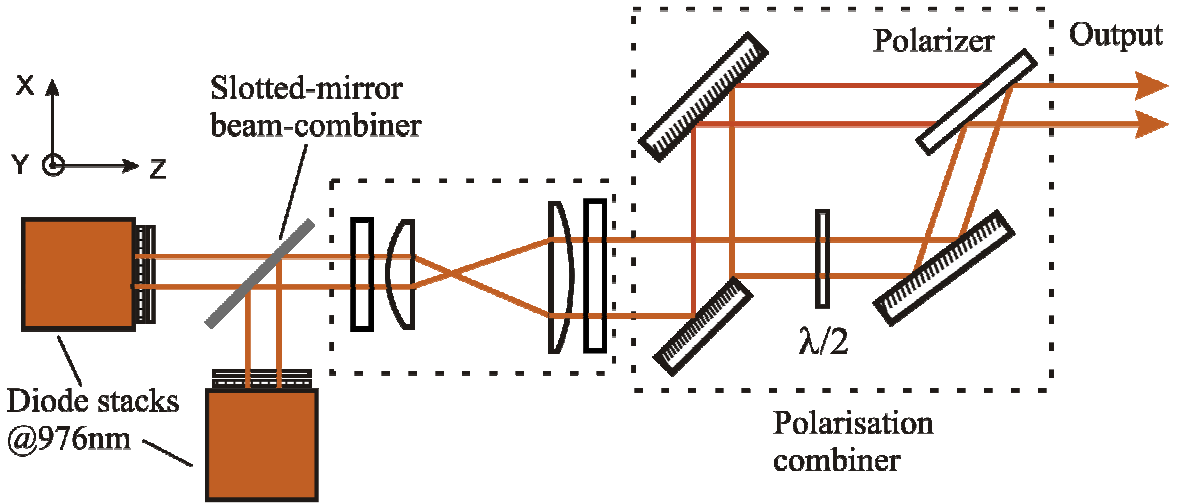


Figure 2: Diode-stack pump source.

the slotted-mirror beam-combiner was then increased by a factor of 2.5 in the x direction and reduced by a factor of 2 in the y direction with the aid of two simple telescopes acting in orthogonal directions (which consisted of two plano-convex cylindrical lenses of focal lengths 100mm and 250mm in x direction, and focal lengths of 200mm and 100mm in the y direction) to produce a beam with transverse dimensions of 25mm and 12mm in the x and y directions respectively. The resulting beam was then split into two beams of equal width in the x direction, which were subsequently polarization-combined to produce a single beam of relatively high-brightness with beam propagation factors of $M_x^2 \sim 200$ and $M_y^2 \sim 150$, and with a maximum power

of ~700 W. The main source of power loss in the system was the slotted-mirror beam-combiner, which, due to imperfect positioning of the constituent mirrors, reduced the power by ~15%. An improved design with more accurate positioning of the mirrors is expected to have a combining efficiency of >95%.

3.3 Er,Yb fiber design

The EYDF used in this project was pulled from a preform fabricated in-house using the standard modified chemical vapour deposition (MCVD) and the solution doping technique [8]. The phospho-silicate core had a diameter of 30 μ m and a numerical aperture (NA) of 0.22 and was doped with Er³⁺ and Yb³⁺. A relatively high Yb³⁺ ion concentration ($\sim 8.7 \times 10^{20} \text{ cm}^{-3}$) was used to achieve a relatively high pump absorption coefficient and to help promote efficient energy transfer from Yb³⁺ to Er³⁺ to increase the overall efficiency. This also helps to prevent parasitic lasing on the Yb³⁺ transition at ~1 μ m. In contrast, a relatively low Er³⁺ ion concentration ($\sim 5.1 \times 10^{19} \text{ cm}^{-3}$) was employed to reduce the re-absorption loss at short wavelengths. The use of a low Er³⁺ ion concentration and a high Yb³⁺ ion concentration is crucial for efficient operation at the short wavelength end of the Er-doped silica emission spectrum in cladding-pumped fiber laser configurations.

The core was surrounded by a pure silica D-shaped inner-cladding of 400 μ m diameter (~360 μ m along the short axis). The latter was coated with a low refractive index (n=1.375) UV curable polymer outer-cladding to produce a high effective numerical aperture (>0.4 NA) waveguide for the pump to facilitate efficient launching of pump light from high-power (but low-brightness) diode sources. The effective absorption coefficient for pump light launched into the cladding as a function of pump wavelength is shown in Fig. 3. It can be seen that the absorption coefficient for pump wavelengths in 974-978nm regime is >6dB/m indicating that relatively short fiber lengths (<3m) would be sufficient for efficient pump absorption. The short device length and the relatively large core diameter of 30 μ m also helps to increase the threshold for unwanted

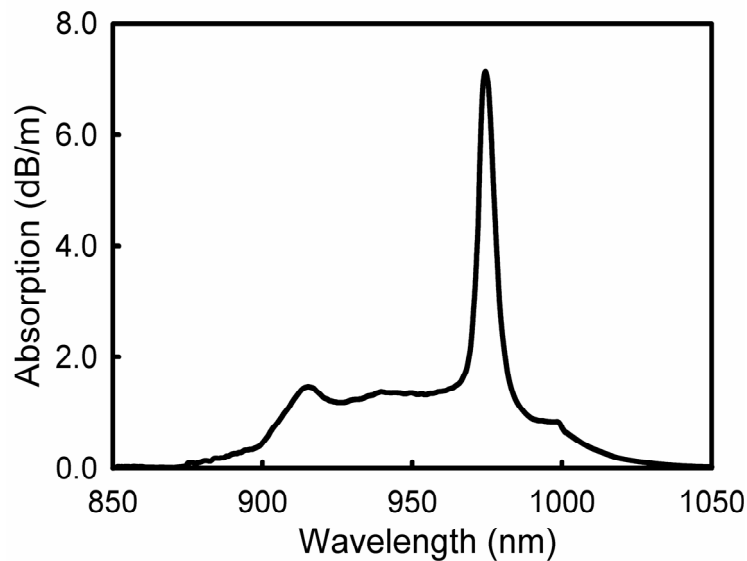


Figure 3: Effective absorption coefficient versus pump wavelength.

nonlinear loss processes, and helps to prevent self-pulsing and damage to the fiber end facets. The use of a diode pump source with emission wavelength closely matched to the absorption peak is therefore very important for efficient operation at 1532nm. Pump wavelengths in the ~920-960nm band would necessitate the use of a longer fiber for efficient pump absorption with the result that there would be reduced gain at shorter wavelengths due to increased re-absorption loss, and amplified spontaneous emission and/or parasitic lasing at longer wavelengths where the gain is higher.

3.4 Er,Yb fiber laser configuration and performance

(a) Single-ended pumping

As a rough guide the upper limit on the pump beam propagation factor, M_{\max}^2 , for efficient coupling into a double-clad fiber of diameter D is given by:

$$M_{\max}^2 \approx \frac{\pi D \sin^{-1}(\text{NA})}{3\lambda} \quad (1)$$

Hence, for efficient coupling into the 400 μm diameter (D-shaped) inner-cladding of our Er,Yb doped fiber, we require $M_{x,y}^2 < 170$. To satisfy this requirement, we reduced the value for M_x^2 from 200 to ~150 by using a simple spatial filter. This also resulted in a reduction in the maximum available pump power to ~520W. This new pumping scheme still offers higher power and much lower M^2 values, as well as improved absorption efficiency, compared to the 940nm diode-stack module used in earlier work.

In preliminary experiments aimed at determining the upper-limit on output power and efficiency for the Er,Yb fiber laser, we employed a very simple (non-tunable) cavity configuration (as shown in Fig. 4). This comprised a ~3m length of EYDF with feedback for lasing provided by an external cavity comprising antireflection coated 50mm focal length collimating and focusing lenses and a plane mirror with high reflectivity (>99.5%) at 1500-1650nm and high transmission (>95%) at 940-980nm, at one end of the fiber and, at the pump in-coupling end of the fiber, by the ~3.6% Fresnel reflection from a perpendicularly-cleaved fiber end-facet. The pump light was launched into the fiber with the aid of a simple two-lens focusing arrangement comprising anti-reflection coated plano-convex lenses with focal lengths 25mm and 40mm, separated by ~30mm, to reduce the detrimental impact of spherical aberration on pump beam quality and launch efficiency. A plane dichroic mirror with high reflectivity (>99.5% at 45°) at the pump wavelength, and high transmission (>98%) at 1530-1570nm was allowed efficient extraction of the EYDF laser (EYDFL) output. In addition, a second dichroic mirror with high reflectivity at 1-1.1 μm and high transmission at 975 nm was inserted into the pump beam (as shown) to prevent any ~1 μm radiation, due to parasitic lasing on the Yb^{3+} transition, from being fed back to the diode-stacks. Using this pumping arrangement, the maximum pump power available at the fiber end facet was 405W, of which ~86% could be launched into the EYDF.

Both end sections of the fiber were carefully mounted in water-cooled V-groove heat-sinks (as

shown in Fig. 4) to prevent thermal damage to the fiber coating due to a small fraction of the pump light leaking into the outer-cladding close to the fiber ends. As an additional precaution against pump-induced damage to the polymer outer-cladding small sections of fiber (~5-10mm

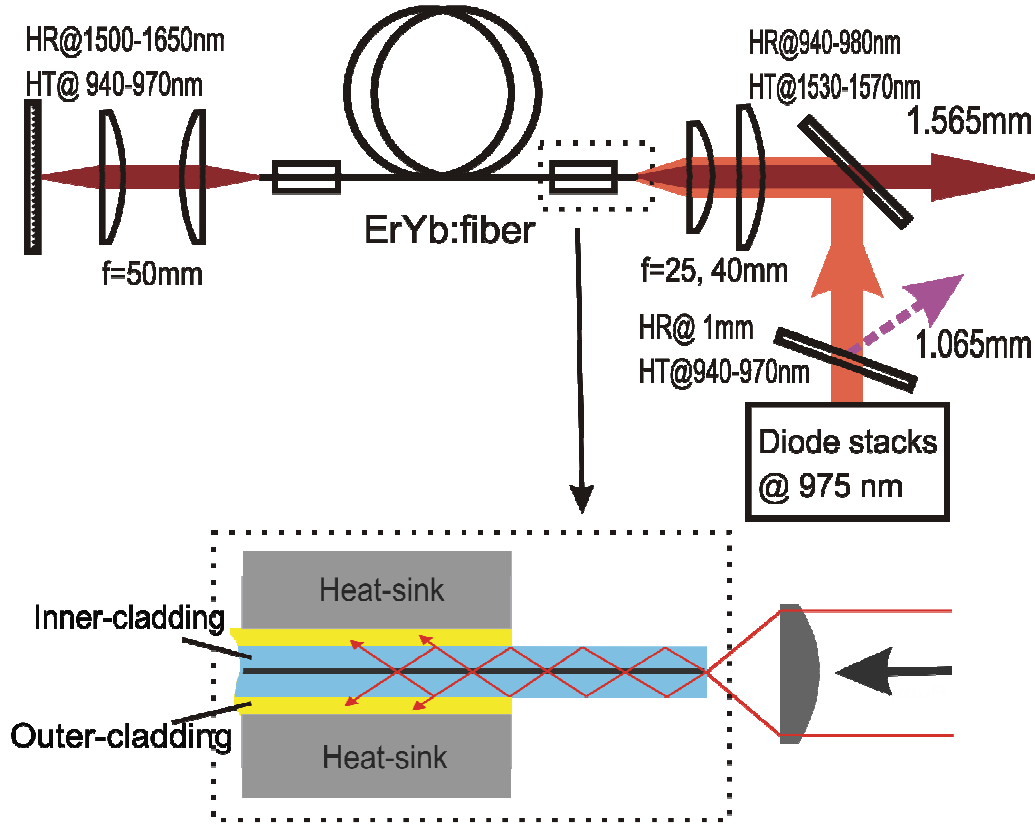


Figure 4: Er,Yb fiber laser configuration for single-ended pumping.

long) with the coating removed were left protruding from the water-cooled V-grooves. In this way, light in the wings of the pump beam (which does not couple directly into the inner-cladding) spreads out rapidly due to diffraction and strikes the water-cooled V-groove and not the polymer outer-cladding.

For the EYDFL configuration shown in Fig. 4, the threshold for lasing was reached at a launched pump power of ~3W and the laser yielded a maximum output power of 129W at 1565nm with a linewidth of ~2.6nm (FWHM) for an incident pump power of 405W (384W launched). The average slope efficiency (with respect to launched pump power) was 37% (see Fig. 5). The slope efficiency decreased slightly at higher powers due to the onset of parasitic lasing on the Yb^{3+} line at 1065 nm. Feedback for ~1 μm lasing was provided by the two perpendicularly-cleaved fiber end facets. Under these operating conditions, the threshold for ~1 μm lasing was reached at a launched pump power of ~125W and the maximum power reached ~23W at a launched pump power of 405W. This indicates that the excitation density for the upper laser level ($^2F_{5/2}$) in Yb^{3+}

increases significantly with pump power which, in turn, suggests that the energy-transfer efficiency from Yb^{3+} to Er^{3+} is sub-optimum. It is also worth noting that the slope efficiency for the EYDFL is somewhat lower than the Stokes efficiency ($\sim 62\%$) and may be explained, at least in part, by a lower than expected energy-transfer efficiency. Thus, with further optimization of

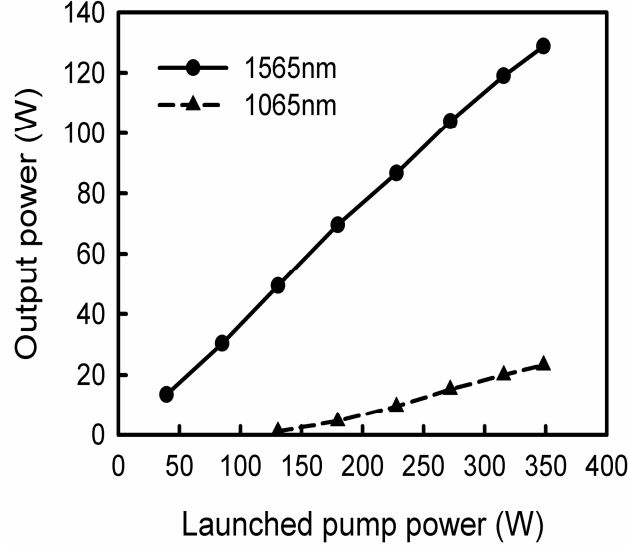


Figure 5: Cladding-pumped Er,Yb fiber laser output power versus launched pump power for single-ended pumping.

the Yb^{3+} and Er^{3+} concentrations it may be possible to achieve a significant increase in the lasing efficiency. The beam quality factor (M^2) for the EYDFL was measured to be 1.9, which was a little better than expected given that the core's V parameter is ~ 13 . The power stability of the laser output was monitored with an InGaAs detector (bandwidth of 50 MHz) and no self-pulsing was observed at all power levels.

(b) Double-ended pumping

The maximum output power for the previous (single-ended pumping configuration) was limited by the maximum pump power that could be launched into the fiber. To increase the launched pump power, and hence the EYDFL output power, a slightly modified pumping scheme was adopted, as shown in Fig. 6. In this arrangement the pump beam from the diode-stack source (described in section 3.2) was split into two beams of roughly equal power and roughly equal M^2 parameters ($M_x^2 \approx 100$ and $M_y^2 \approx 150$) using a plane mirror with high reflectivity at the pump wavelength. Pump light was then launched into opposite ends of the EYDF with the aid of anti-reflection coated focusing lenses of 25mm focal length and dichroic mirrors with high reflectivity ($>99.5\%$ at 45°) at the pump wavelength, and high transmission ($>98\%$) at 1530-1570nm. As before, dichroic mirrors with high reflectivity at 1-1.1 μm and high transmission at 975 nm were inserted into both pump beams (as shown in Fig. 6) to prevent any $\sim 1 \mu\text{m}$ radiation, due to parasitic lasing on the Yb^{3+} transition, from being fed back to the diode-stacks. For this pumping scheme, we estimated that the overall launch efficiency into the fiber with respect to incident pump power was $\sim 80\%$, and hence a little lower than for the two-lens focusing

arrangement shown in Fig. 4. However, in this case it was not necessary to use a spatial filter to improve the beam quality before the final focusing lenses, hence a much higher combined incident pump power ($\sim 582\text{W}$) was available, of which $\sim 466\text{W}$ could be launched into the EYDF. The EYDFL resonator design employed was identical to that used for single-ended

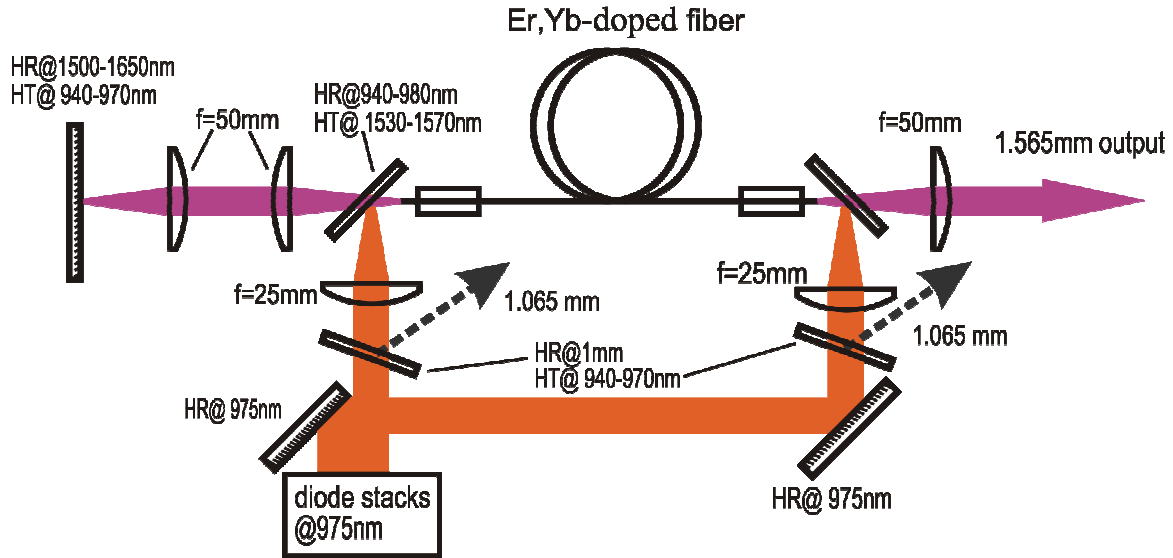


Figure 6: Er,Yb fiber laser configuration for double-ended pumping.

pumping, except for the addition of a dichroic mirror in the external feedback cavity to allow coupling of pump light into the adjacent fiber end-facet as well as the opposite fiber end-facet. With this improved pumping scheme, the EYDFL yielded a maximum output power of 159W at 1565nm at the maximum pump power, corresponding to an average slope efficiency of $\sim 34\%$ (see Fig. 7). The EYDFL had a higher slope efficiency of 37% at low pump powers ($<220\text{W}$), which decreased to 31% at high pump power due to the onset of parasitic lasing on the Yb^{3+} transition at $\sim 1\mu\text{m}$. The combined output (i.e. from both fiber ends) at $1.065\mu\text{m}$ was measured to be $<28\text{W}$. Clearly, it is important to suppress the $1\mu\text{m}$ lasing to realize efficient operation at $\sim 1.5\mu\text{m}$. One way to avoid parasitic lasing at $\sim 1\mu\text{m}$ is to increase the cavity loss at $\sim 1\mu\text{m}$ by using an angle-polished fiber end facet nearest the external cavity and by using an external cavity mirror with high transmission in the $1\mu\text{m}$ regime. It is worth noting that the combined laser output power at $1.565\mu\text{m}$ and $1.065\mu\text{m}$ (shown in Figs. 5 and 7) increases more or less linearly with pump power at even the highest pump power available, and there is no evidence of any detrimental impact due to thermal loading. Hence, with the appropriate cavity design and with the required degree of suppression of $1\mu\text{m}$ lasing, it should be possible to obtain a further increase in output power at $\sim 1.5\mu\text{m}$ by simply increasing the pump power.

Removing the high reflectivity mirror from the external cavity, so that feedback for both $1\mu\text{m}$ and $1.57\mu\text{m}$ lasing was provided by the two perpendicularly-cleaved fiber end facets, resulted in a combined output power of 188W at 1565nm for a launched pump power of 466W (see Fig. 8).

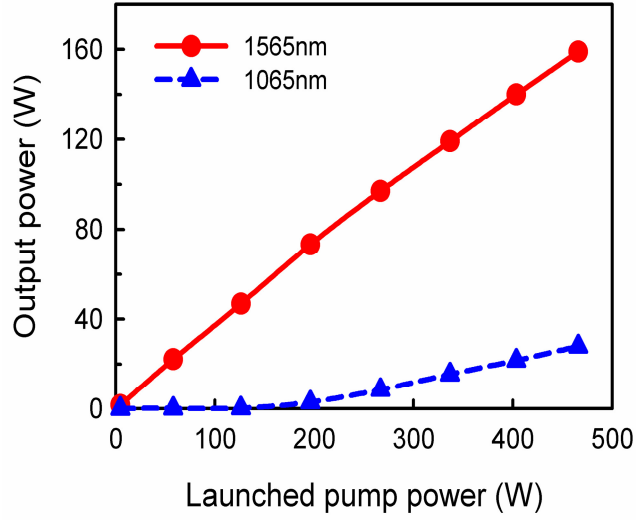


Figure 7: Output power versus launched pump power for free-running Er,Yb fiber laser with double-ended pumping

The overall slope efficiency with respect to launched pump power was 41%. Similarly, the laser exhibited a high slope efficiency of 43.1% at low pump powers ($< 300\text{W}$), which decreased to 36.8% at high pump powers due, once again, to lasing on Yb^{3+} transition. In this case, lasing at 1065nm resulted in a total output power (i.e. from both fiber ends) of $< 20\text{W}$. It is interesting to

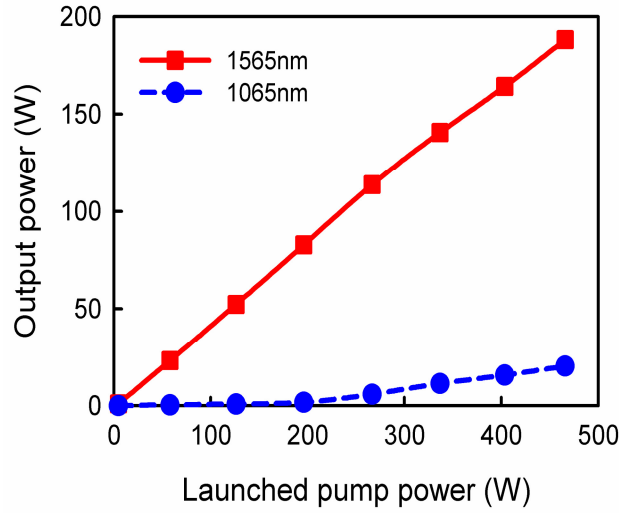


Figure 8: Output power versus launched pump power with no external cavity.

note that the $1\mu\text{m}$ power was significantly lower for the latter cavity configuration. This is believed to be due to lower cavity losses at $1\mu\text{m}$ for the former cavity configuration (shown in

Fig. 6) due to residual feedback from the external feedback cavity at $\sim 1\mu\text{m}$. The laser output power versus pump power (see Fig. 8) is still more or less linear even the highest pump powers if parasitic lasing at $\sim 1\mu\text{m}$ is taken into account, with no evidence of decrease in efficiency due to thermal loading. Hence, with more pump power it should be possible to obtain a further increase in output power.

3.5 Tunable Er,Yb fiber laser

Tunable operation of the EYDFL was demonstrated employing a simple external cavity design, as shown in Fig. 9, comprising an antireflection coated collimating lens of focal length 120 mm

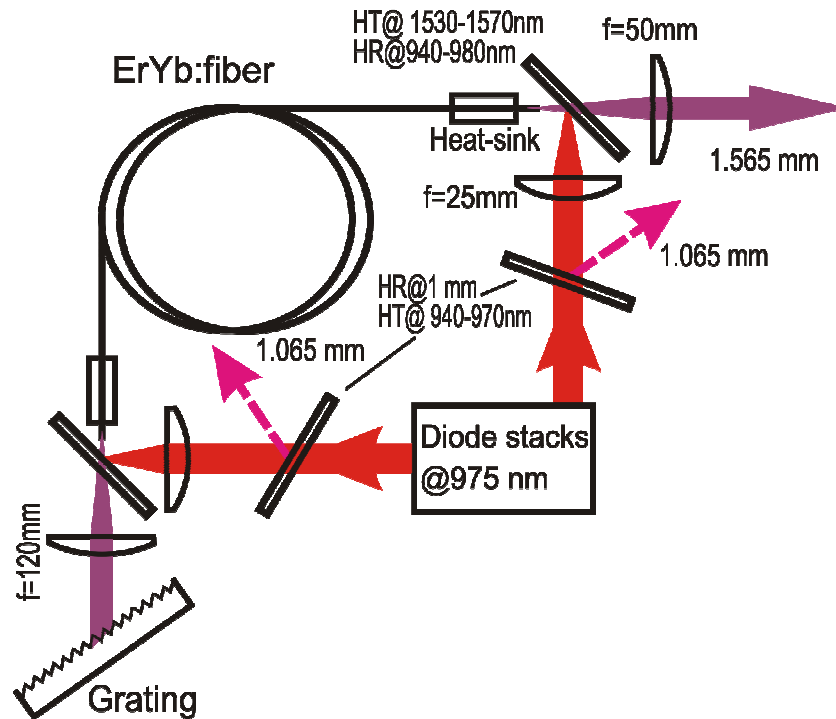


Figure 9: Tunable Er,Yb fiber laser configuration.

and a simple replica diffraction grating (600 lines/mm) mounted on a copper substrate to facilitate removal of waste heat. A relatively long focal length collimating lens in the external feedback cavity was selected to avoid any possible damage to the grating, and to reduce the collimated beam divergence and hence increase the spectral selectivity of the grating feedback cavity. The grating was blazed for wavelength of $\sim 1.65\mu\text{m}$ with reflectivity of $\sim 75\%$ for light polarised parallel to the grooves and $\sim 95\%$ for light polarised in the orthogonal direction, and was aligned in the Littrow configuration to provide wavelength selective feedback and hence the means for adjusting the lasing wavelength. The fiber end facet nearest the grating was angle-polished at $\sim 14^\circ$ to suppress parasitic lasing between the two fiber end facets. A shorter fiber length of $\sim 2\text{m}$ was selected for the tunable operation and the combined unabsorbed pump power

(from two ends) was measured to $< 7\text{W}$ for a total launched pump power of 336W . In this experiment, the maximum launched pump power was limited to $\sim 336\text{W}$ to minimize the risk of thermally-induced damage to the polymer coating and/or fiber end section. Using this resonator configuration, the laser generated a maximum output power of 108W at 1538 nm for $\sim 336\text{W}$ of launched pump power (see inset of Fig. 10). The threshold pump power (launched) was $\sim 3.3\text{W}$ and the slope efficiency with respect to launched pump power was 32% . The linear dependence of the output power on the pump power suggests that there was no severe thermal induced deformation on the bulk grating even at highest pump power, and indicates that there is scope for further power scaling of this simple tunable EYDFL laser architecture. The laser output power as a function of operating wavelength is shown in Fig. 10. The lasing wavelength could be tuned

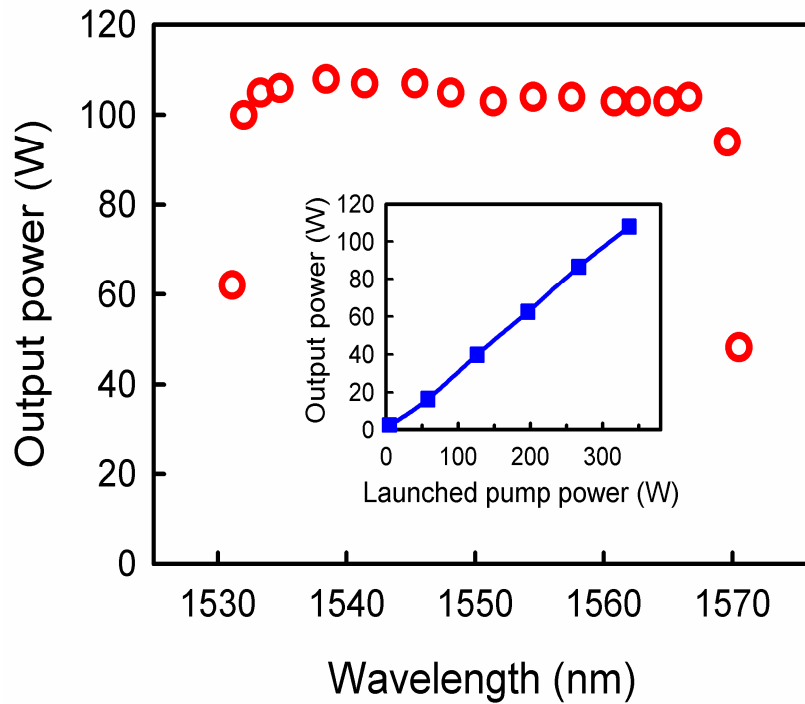


Figure 10: Tunable Er,Yb fiber laser output power versus operating wavelength for a 2m fiber. (Inset: Output power of the tunable Er,Yb fiber laser at 1538nm versus launched pump power).

from 1531 to 1571nm at output power levels $> 50\text{W}$, and over 36 nm from ~ 1532 to 1568nm at output power levels in excess of 100W . The linewidth (FWHM) was $\sim 1\text{ nm}$ and the short-term power stability was measured to be $< 0.9\%$ (RMS) on a timescale of $300\mu\text{s}$. The output power was also very stable over longer time periods with power fluctuations of $< 3\%$ over a timescale of 30 minutes. Moreover, we did not observe any degradation in performance over a period of several months of intermittent use. Further details of this work can be found in Appendix A1.

3.6 Thermal effects and their mitigation

The maximum output powers for the EYDFL configurations discussed in the previous sections were limited by available pump power. However, in preliminary experiments, thermally-induced damage to the protruding fiber end sections and/or polymer coating limited the EYDFL output power. Thermally-induced damage was avoided by carefully selecting the length of fiber protruding from the heat-sinks, and by careful design of the water-cooled heat-sink. The main damage mechanism is thought to be melting of the core and surrounding material due to heat generated in the core, and the main source of waste heat is thought to be quantum defect heating. An estimate of the maximum heat that can be generated per unit length of fiber $(P_h/L)_{\max}$ before the onset of melting can be obtained from [9]

$$\left(\frac{P_h}{L}\right)_{\max} \approx \frac{4K_c(T_m - T_c)}{\left[1 + \frac{2K_c}{bh} + 2\log_e\left(\frac{b}{a}\right)\right]} \quad (2)$$

where a is the core radius, b is the inner-cladding radius, K_c is the thermal conductivity of silica, T_m is the melting/softening temperature of silica ($\sim 2000\text{K}$), T_c is the ambient temperature of the surroundings and h is the heat transfer coefficient. This assumes that the heat flow is purely radial, which is usually a reasonable approximation for a fiber-based source. Figure 11 shows calculated values for $(P_h/L)_{\max}$ for the protruding section of our EYDF as a function of the heat

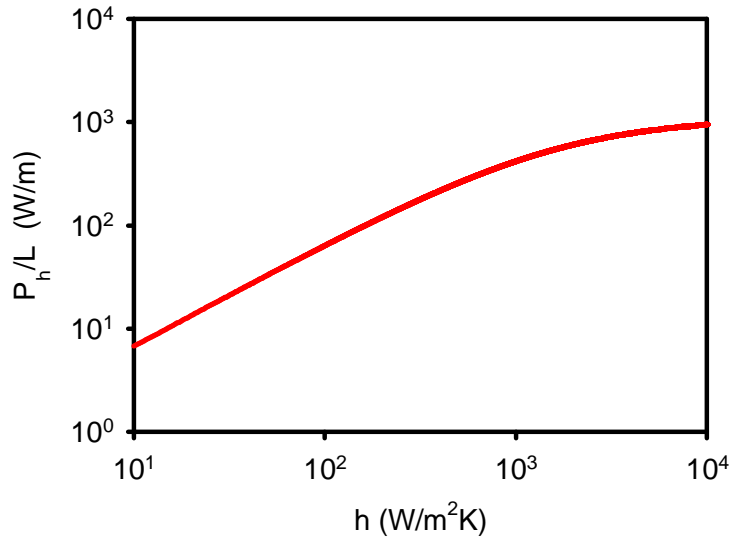


Figure 11: Heat per unit length (P_h/L) versus heat transfer coefficient (h)

transfer coefficient. The actual value for the heat generated per unit length of fiber (P_h/L) is given by

$$\left(\frac{P_h}{L}\right) \approx \alpha_p \gamma_h P_p(z) \quad (3)$$

where α_p is the pump absorption coefficient, γ_h is the fraction of absorbed pump light converted to heat and $P_p(z)$ is the pump power in the fiber at position z . If we assume that heat is generated by quantum defect heating (i.e. $\gamma_h=0.36$), then for the single-ended pumping arrangement (P_h/L) $\approx 190\text{Wm}^{-1}$ at the input end of the fiber. This suggests that the heat transfer coefficient (h) must be $>340\text{Wm}^{-2}\text{K}^{-1}$, otherwise the fiber would melt. The value for h is strongly dependent on the operating conditions. Even a small amount of forced-air cooling can yield a much higher value for h . In our set-up, the end of the fiber was cooled using a fan. A further improvement in the fibers thermal handling capability could be achieved by using a larger diameter fiber with increased surface area for cooling, or by using an undoped end-cap and conduction cooling the active (doped) section of fiber.

3.7 Prospects for further power scaling

From the above discussion it is clear that there is still a great deal to be gained in terms of power scalability by improving thermal management. In addition, higher power and higher brightness pump sources will be needed. The upper-limit on launched pump power based on the brightness of an individual diode emitter for a perfect pump collection, re-shaping and delivery optical arrangement (without polarization or wavelength multiplexing) is $>4\text{kW}$ for a $400\mu\text{m}$ diameter fiber. This is far beyond the current state-of-the-art and the launched pump power in our experiments, so there is plenty scope for improvement. Moreover, we also believe that there is still scope for improvement in the lasing efficiency. We have demonstrated slope efficiencies with respect to absorbed pump power $>40\%$, which are comparable with the best that have been reported for EYDFL's, but this is still somewhat lower than the quantum limit. Further optimization of the Yb^{3+} and Er^{3+} ion concentrations, and the core composition may well yield a further increase in efficiency and help to suppress parasitic lasing.

4.0 Tm FIBER SOURCE

4.1 Introduction

Cladding-pumped Tm-doped fiber lasers operating in eye-safe $2\mu\text{m}$ spectral region have attracted enormous interest in recent years owing to their numerous applications. A particular attraction of Tm-doped fiber lasers is the very broad transition linewidth offering the prospect of wide tunability over the $\sim 1700\text{-}2100\text{nm}$ regime. Another attractive feature of Tm-doped silica fibers is that there are a number of different options for pump sources owing to absorption bands

in the $\sim 0.8\mu\text{m}$, $\sim 1\text{-}1.3\mu\text{m}$ and $\sim 1.5\text{-}1.6\mu\text{m}$ wavelength regimes (see Figs. 12 and 13). There is a strong absorption line at $\sim 1.2\mu\text{m}$, corresponding to the $^3\text{H}_6 - ^3\text{H}_5$ transition, but this wavelength

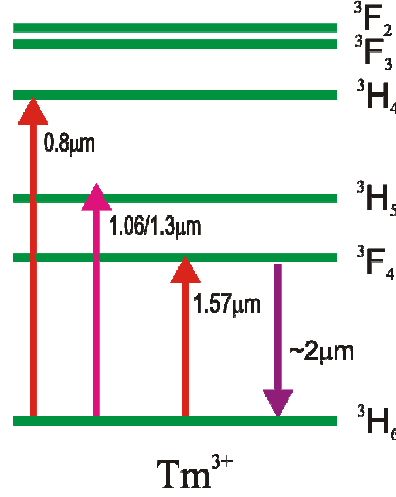


Figure 12: Pump schemes for Tm^{3+} doped fibers.

is rather difficult to obtain. The wings of this absorption line extend to $\sim 1\mu\text{m}$ and $\sim 1.3\mu\text{m}$ making Yb or Nd lasers candidate pump sources. However, the absorption is relatively weak at these wavelengths and is further complicated by the presence of strong excited-state absorption (ESA) at $\sim 1\mu\text{m}$ (see Fig. 14(a)). As a result, efforts to power scale Tm fiber lasers by pumping at these wavelengths have yielded rather low efficiencies and low output power [10-12].

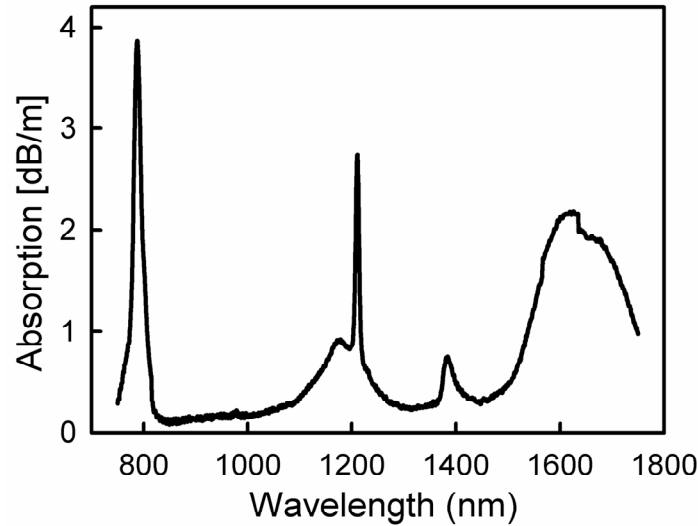


Figure 13: Absorption spectrum for Tm^{3+} -doped silica.

Tm^{3+} has a level ($^3\text{H}_5$) which is quasi-resonant with the excited Yb^{3+} level $^2\text{F}_{5/2}$, allowing for the possibility of sensitization of Tm^{3+} -doped fibers with Yb^{3+} . In a Tm^{3+} - Yb^{3+} co-doped fiber, Yb^{3+} ions are pumped by near-infrared diodes and then energy is transferred non-radiatively to the Tm^{3+} ions, which can then emit in the $2\mu\text{m}$ wavelength range (see Fig. 15). This makes it possible to use commercially available high-power pump diodes in the 910–980nm regime. So far, up to 75W (limited by fiber damage) has been generated via this pumping scheme, but with rather low slope efficiencies ($\sim 32\%$ [13]), due, in part, to relatively high quantum defect heating ($\sim 51\%$). Hence, power scaling via this approach may prove rather difficult. At the time this project commenced, direct pumping of double-clad Tm-doped silica fiber lasers with diode lasers at $\sim 790\text{ nm}$ had yielded output power up to 14W (limited by available pump power [1]). It has been shown that slope efficiencies beyond the Stokes limit ($\sim 39\text{-}40\%$) can be achieved in Tm^{3+} -doped silica fiber lasers by using a high Tm^{3+} concentration to promote the cross-relaxation process, $^3\text{H}_4, ^3\text{H}_6 \rightarrow ^3\text{F}_4, ^3\text{F}_4$ (see Fig. 14 (b)) [14]. This is an attractive pumping scheme for power scaling owing to the availability of high power diodes and the prospect of very high efficiencies, but the low brightness of the diode pump sources has so far limited operation to wavelengths $>1850\text{nm}$.

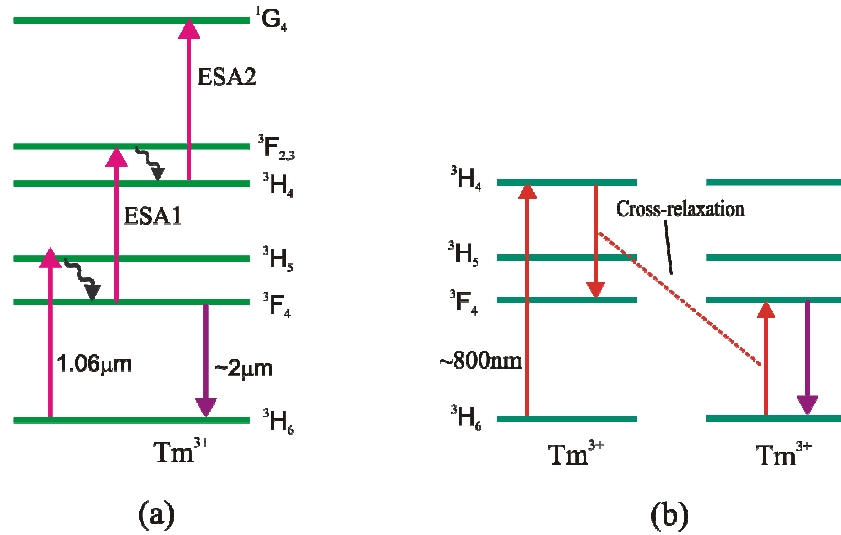


Figure 14: Energy levels of the Tm^{3+} ion in silica.

An alternative, and more promising, approach for power scaling of Tm fiber lasers is to pump directly into the upper level manifold ($^3\text{F}_4$) with an Er fiber laser at $1.55\text{-}1.62\mu\text{m}$. This approach has the attraction of a very high Stokes efficiency ($\sim 0.75\text{-}0.85$) and hence low quantum defect heating, opening up the prospect of very high lasing efficiencies. Moreover, the good beam quality available from high-power Er-doped fiber lasers allows direct pumping into the Tm-doped fiber core leading to the possibility of a much shorter device length. This is crucial for extending the tuning range of Tm fiber lasers to the shorter wavelength region. Tm-doped fibers with low output power ($<20\text{mW}$), pumped near $1.6\mu\text{m}$, with slope efficiency as high as 71% (for silica fibers [15]) and 84% (for fluoride fibers [16]) have been reported previously. As far

as we are aware, this approach for power scaling of Tm-doped fiber lasers has not attracted much interest, perhaps, because it requires a high power Er,Yb fiber source.

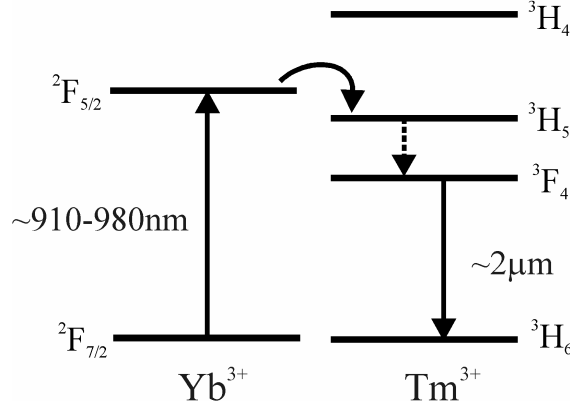


Figure 15: Energy level diagram of Yb³⁺ and Tm³⁺ ions in silica.

4.2 Tm fiber design

Tm-doped fibers with two different sets of design parameters were used in our study. One was pulled from a preform (F95-HD510) fabricated in-house using the standard chemical-vapour deposition and solution-doping technique. The resulting perform had a thulium concentration of ~1.3% by weight. To improve pump absorption, the inner-cladding was shaped to break the symmetry of the fiber (see Fig. 16). The latter was achieved by milling two flats inclined at 28° with respect to each other on the preform prior to pulling the fiber. The resulting fiber had a Tm-

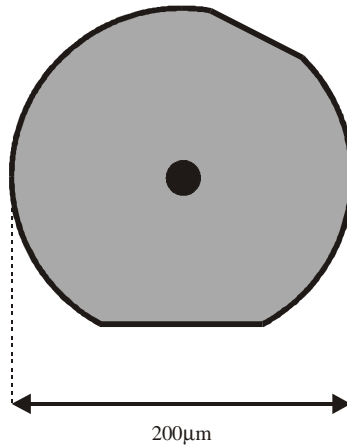


Figure 16: Double-clad Tm-doped silica fiber.

doped alumino-silicate core of diameter of 20μm with a numerical aperture (NA) of 0.12, and an inner cladding of outer dimension 200μm. The latter was coated with a low refractive index

($n=1.357$) polymer outer-cladding resulting in a nominal numerical aperture of 0.49 for the inner-cladding pump guide. In practice, the effective NA of the inner-cladding was a little lower (~ 0.4). The relatively small inner cladding size was originally chosen to minimize the cladding-to-core area ratio to maximise pump absorption, while allowing efficient in-coupling of the diode pump light at $\sim 790\text{nm}$. The small cladding-to-core area ratio (<100) is also beneficial for $1.57\mu\text{m}$ (in-band) pumping since the absorption coefficient at this wavelength is lower than at $\sim 790\text{nm}$. The effective absorption coefficient (i.e. for cladding-pumping) at 790nm for this fiber was estimated (via a cut-back measurement) to be $\sim 4\text{dB/m}$ (see Fig. 13). A second Tm-doped fiber was also used in our study. This fiber had an $18\mu\text{m}$ diameter (0.24 NA) alumino-silicate core with a very high Tm doping level of $\sim 2.2\text{wt}\%$. The core was surrounded by a D-shaped pure silica inner-cladding of diameter $\sim 300\mu\text{m}$ with a polymer outer-cladding and an effective NA of ~ 0.3 . The high Tm^{3+} concentration was used to promote ‘two-for-one’ cross-relaxation in order to increase the pumping quantum efficiency when pumping at $\sim 0.8\mu\text{m}$. In addition a high $\text{Al}^{3+}/\text{Tm}^{3+}$ ion concentration ratio of ~ 8 was employed to reduce the degree of ion clustering and hence ensure efficient operation. The effective absorption coefficient at 790nm for this fiber was determined to be $\sim 6\text{dB/m}$. A further attraction of using a high Tm^{3+} concentration is that it allows efficient pump absorption in a short length of fiber, thereby reducing the core background propagation loss and increasing the threshold for unwanted nonlinear loss processes.

4.3 Pumping geometries: Cladding versus core pumping

Cladding-pumping of fiber lasers and amplifiers is now a very well established technique for scaling fiber output powers with high power, but low brightness diode pump sources. In a cladding-pumped fiber configuration, the effective pump absorption coefficient is roughly equal to the absorption coefficient in the core divided by the ratio of the inner-cladding area to core area. Thus, the absorption coefficient in a double-clad fiber is many times smaller than for pump light in the core. As a result, the length of fiber required for efficient pump absorption in a cladding-pumped scheme is typically rather long. As fiber power levels rise, the need for larger inner-cladding sizes to accommodate more pump power results in a further reduction in the absorption coefficient, and hence even longer fiber are needed. This pushes the gain spectrum to longer wavelengths and makes it increasingly difficult to force the laser to operate at short wavelengths. In contrast, core pumping provides much more flexibility and access to much shorter operating wavelengths by virtue of the much stronger pump absorption. However, core pumping does require a much higher brightness pump source. Tm-doped silica fiber lasers can be pumped by high power Er,Yb fiber sources in either cladding or core-pumped configurations. Figure 17 shows a typical lasing spectrum of a free-running cladding-pumped Er,Yb fiber lasers together with the effective absorption coefficient versus wavelength (i.e. for cladding pumping) in the Tm-doped fiber pulled from preform F95-HD510. It can be seen that the absorption maxima is at $\sim 1630\text{nm}$ and hence is a little beyond the maximum operating wavelength of an EYDFL. However, the effective absorption coefficient is still relatively high ($\sim 1.7\text{dB/m}$) at the EYDFL operating wavelength ($\sim 1.56\mu\text{m}$). This is only a factor-of-two smaller than pump light at $\sim 790\text{nm}$. Thus, cladding-pumping at $\sim 1.56\mu\text{m}$ should be very efficient. It is worth pointing out that the beam quality from the EYDFL is far superior to that of a high power laser diode, so a much smaller cladding size could be employed with obvious benefits to laser performance. From Figure 17 we estimate that the core absorption coefficient in the Tm doped fiber at the EYDFL operating wavelength is $\sim 170\text{dB/m}$. If ground-state depletion is neglected, this would

suggest that the length of fiber required in a typical core-pumped laser (using the same Tm fiber composition) could be ~5cm. However, such a laser would probably need very efficient heat-sinking to prevent damage at high pump powers.

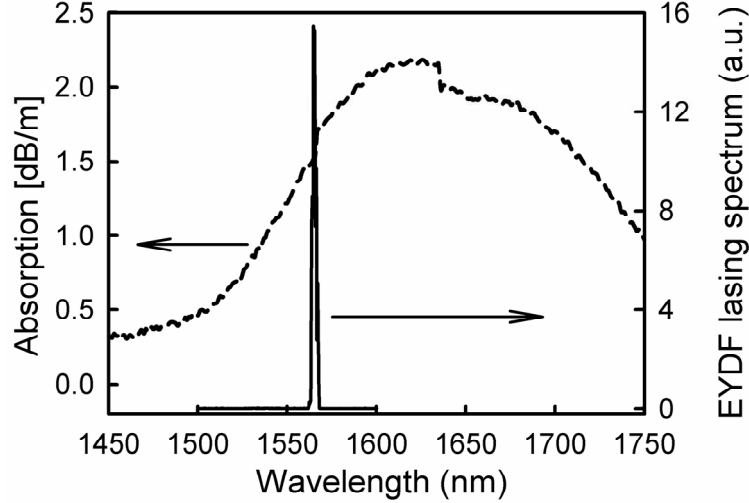


Figure 17: Effective absorption coefficient for Tm fiber (from F95-HD510) and output spectrum of the EYDFL.

4.4 Cladding-pumped Tm fiber lasers: 790nm versus 1565nm pumping

(a) Pumping at 790nm

The low doping level Tm fiber from preform F95-HD510 (fiber (A)) was first tested by pumping with two beam-shaped diode-bar pump sources at 790nm. These provided pump powers of 25W and 30W in beams with roughly equal M^2 parameters in orthogonal planes (i.e. $M_x^2 \approx M_y^2 \approx 70$). The fiber laser was pumped through opposite ends using dichroic mirrors (M1, M2), with high reflectivity at the pump wavelength (785-795nm) and high transmission at the lasing wavelength (1850-2100nm) at 45°, to separate pump and signal beams (see Fig. 18). This arrangement allows the use of different lenses for collimating the fiber laser output and focusing the pump, and hence has the advantage that the resonator alignment and pump launching optics can be independently optimised. With the above setup, ~80% of the incident pump power was launched into the fiber. A relatively simple fiber laser configuration was employed consisting of a ~4.7m length of Tm fiber with feedback for lasing provided by an external cavity comprising antireflection coated 25mm focal length collimating lens and a plane mirror with high reflectivity (>99.5%) at 1800-2100nm and high transmission (>95%) at 780-800nm, at one end of the fiber and, at the opposite (out-coupling) end of the fiber, by the ~3.6% Fresnel reflection from a perpendicularly-cleaved fiber end-facet. The fiber-end nearest the external cavity was angle-polished at 8° to suppress broadband feedback from the uncoated face so that the set-up could easily be modified for tunable operation. Wavelength tuning was achieved by replacing the high reflection mirror in the external cavity with a simple diffraction grating with 600 lines/mm

aligned in the Littrow configuration to provide wavelength selective feedback. The grating was blazed at wavelength of $1.9\mu\text{m}$ and had measured reflectivities of 90% (for light polarised perpendicular to the grooves) and 70% (for light polarised parallel to the grooves) at $2\mu\text{m}$. A longer fiber ($\sim 4.7\text{m}$) than would be optimum was used to ensure that negligible pump light was transmitted by the fiber as a precaution against damage to opposing diodes.

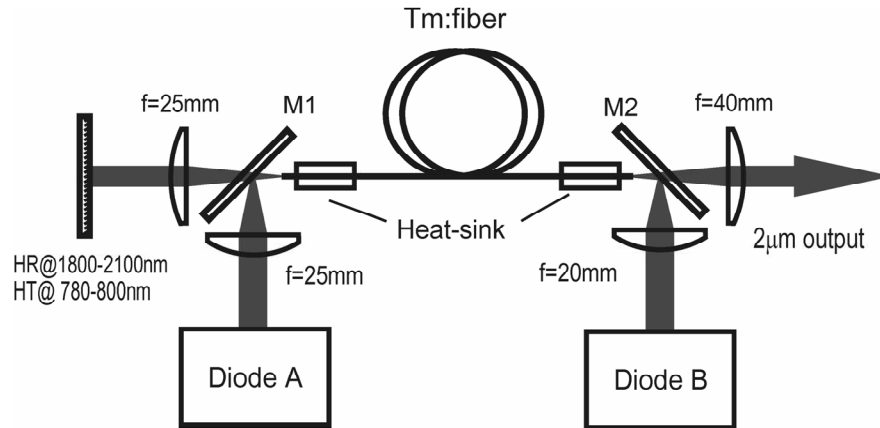


Figure 18: Schematic diagram of the Tm fiber laser cladding-pumped by 790nm diode-bars

For free running operation (i.e. with no wavelength selection) the threshold pump power incident on the pump focussing lens was measured as $\sim 7.5\text{W}$ ($\sim 6\text{W}$ launched), and at the maximum available incident pump power of 55W (corresponding to $\sim 44\text{W}$ launched) the fiber laser produced a maximum output power 11.4W at $\sim 1925\text{nm}$ (see Fig. 19) corresponding to an average slope efficiency with respect to launched pump power of $\sim 30\%$. At the highest pump

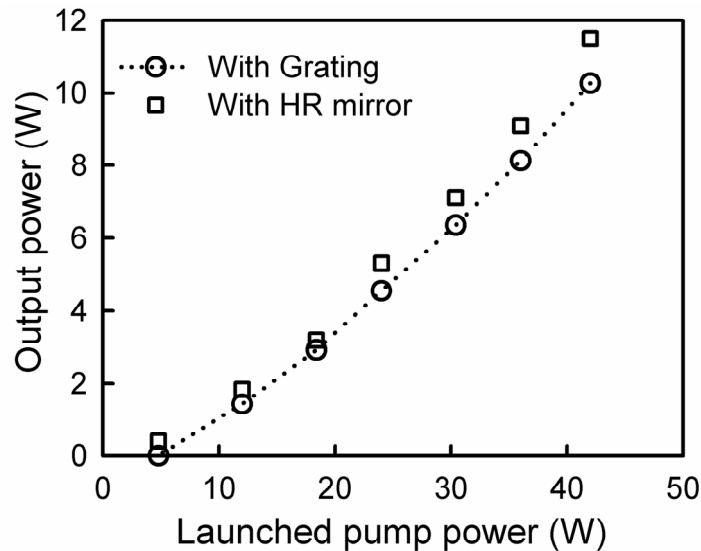


Figure 19: Tm-fiber laser output versus launched pump power at 790nm.

powers the slope efficiency increases to ~36%. This suggests that by using higher power diode-bars, it should be possible to achieve a significant increase in optical-to-optical efficiency as well as higher output power. By taking into account the effect of spherical aberration on beam quality, we estimate that $M^2 \approx 1.4$ for the fiber output (i.e. before the collimating lens). The use of aberration-corrected lenses should improve the beam quality and, in addition, may help to improve performance and extend the wavelength tuning range by increasing the feedback efficiency of the external cavity. When the high reflectivity mirror in the external cavity was replaced by the diffraction grating, a slightly lower output of 10.3W was obtained at ~44W of launched pump power (see Fig. 19). The lasing wavelength could be tuned, by a simply adjusting the grating angle, over 215nm from 1855 to 2070nm at multi-watt power levels, and over 150nm from ~1860 to 2010nm at output power levels in excess of 9W (see Fig. 20). The bandwidth of the tunable laser output (FWHM) was ~1nm.

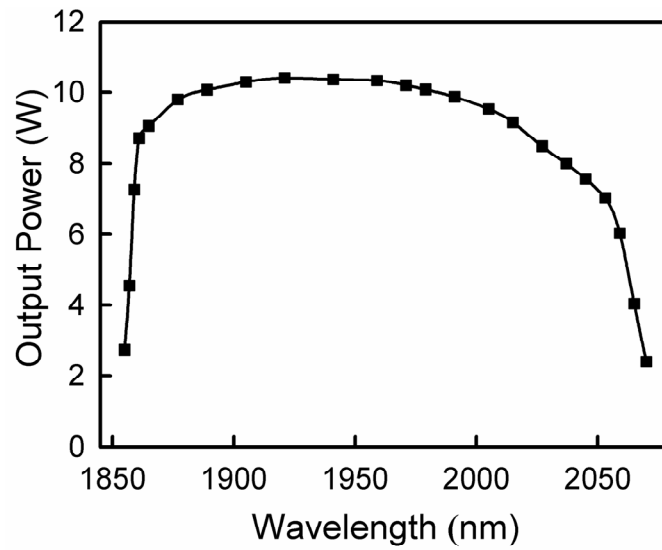


Figure 20: Tunable Tm fiber laser output power versus operating wavelength.

Cladding-pumping of the high-doping level Tm fiber (fiber B) with 790nm diodes was also investigated. A schematic diagram of the laser configuration is shown in Fig. 21. A very simple resonator configuration was employed with feedback for lasing provided by a plane mirror with high reflectivity (>99%) at 1850-2100nm and high transmission at the pump wavelength ($T > 97\%$ at 790nm) butted to one end of the fiber, and by the 3.6% Fresnel reflection from a perpendicularly-cleaved facet at the opposite end of the fiber. The latter served as the output coupler with its high transmission dominating over other cavity losses. The two diode-bars were polarization-combined and the resulting beam was re-formatted with the aid of a two-mirror beam-shaper, to produce a beam with beam propagation factors in orthogonal planes of $M_x^2 \approx 80$ (parallel to the array) and $M_y^2 \approx 52$ (perpendicular to the array) and a maximum power of ~52W at 790nm. The pump light was coupled into the output end of the Tm-doped fiber using a 30mm aspheric focusing lens, and a dichroic mirror with high reflectivity (>98%) at 790nm and high transmission (>97%) at 1800-2100nm at 45° was used to allow extraction of the two-micron fiber laser output. Using this arrangement, a maximum combined pump power of 44W was

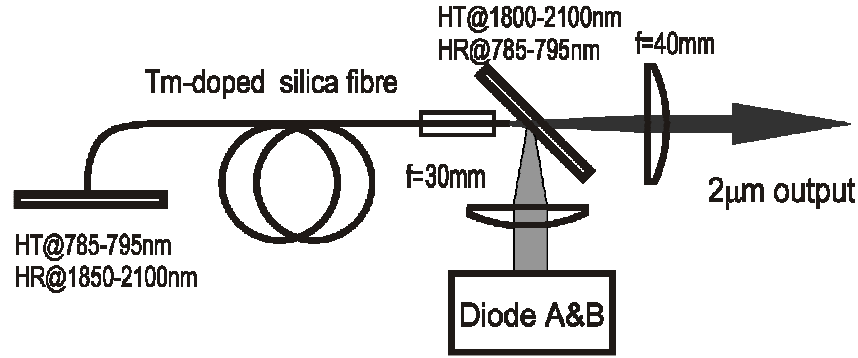


Figure 21: Tm-doped silica fiber laser set-up with single-ended pumping.

launched into the fiber corresponding to a launch efficiency of 85%. The unabsorbed 790nm pump light was monitored at the other end of the fiber. The output power as a function of both launched and absorbed pump power is plotted in Fig. 22. The best performance in terms of output power and slope efficiency was obtained from the 2.2m length of fiber. This produced a

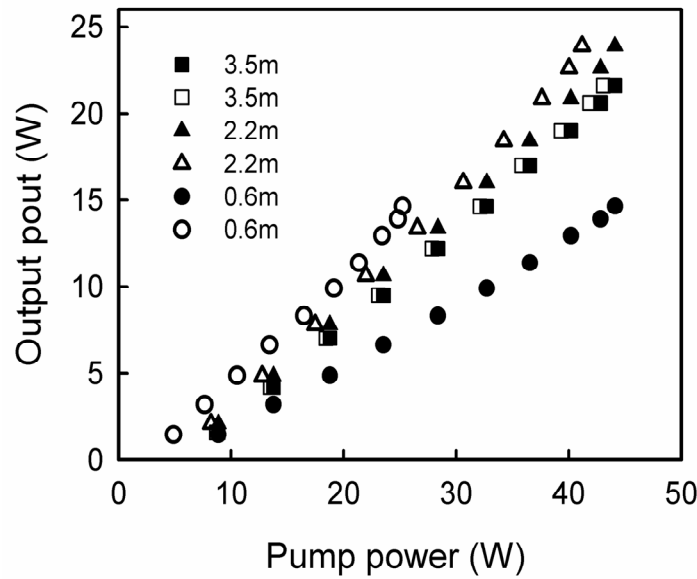


Figure 22: Tm fiber output power versus pump power for 0.6m (circle), 2.2m (triangle) and 3.5m (square) fiber lengths. Data plotted in filled and open symbols are with respect to launched and absorbed pump power respectively.

maximum output power of 23.9W at 2025nm for an incident pump power of 44.1W, corresponding to a slope efficiency with respect to launched and absorbed pump power of 61.1% and 65.2% respectively. A slightly lower output power of 21.6 W at 2042 nm was generated for the same launched pump power from the 3.5m fiber with lower slope efficiency and an increased threshold due to increased re-absorption loss and higher background propagation loss in the core (see Table 1). The 0.6m Tm fiber yielded a slope efficiency with respect to absorbed pump

power of 62.8%, which is a little lower than expected. This is believed to be due to slightly higher cavity loss resulting from an imperfect fiber end-facet.

Fiber length (m)	λ (nm)	Slope efficiency (%)		P_{th} (W)	P_{out} (W)
		wrt P_{launch}	wrt P_{abs}		
0.6	1990	37.0	62.8	3.0	14.6
2.2	2025	61.1	65.2	4.9	23.9
3.5	2042	56.5	57.8	5.7	21.6

Table 1. Summary of the Tm fiber laser performance versus fiber length

(b) Pumping at 1565nm

Cladding-pumping of Tm fiber (A) with the 1.565 μ m Er,Yb fiber laser was also investigated. The effective absorption coefficient for cladding pumping at 1565nm was measured (via a cut-back measurement) to be ~ 1.7 dB/m. Schematic diagrams of cladding-pumped Tm fiber configurations used in this study are shown in Fig. 23. Pump light at 1565nm laser from the EYDFL was launched into the Tm fiber using a 50mm focal length lens anti-reflection coated at $\sim 1.5\mu$ m. The launch efficiency was estimated to be $\sim 86\%$. Both end sections of the fiber were mounted in water-cooled V-groove heat-sinks to prevent possible thermal damage to the fiber coating by pump power which overfills the inner-cladding NA, and by heat generated in the core due to quantum defect heating. The laser cavity for free-running operation (shown in Fig. 23(a))

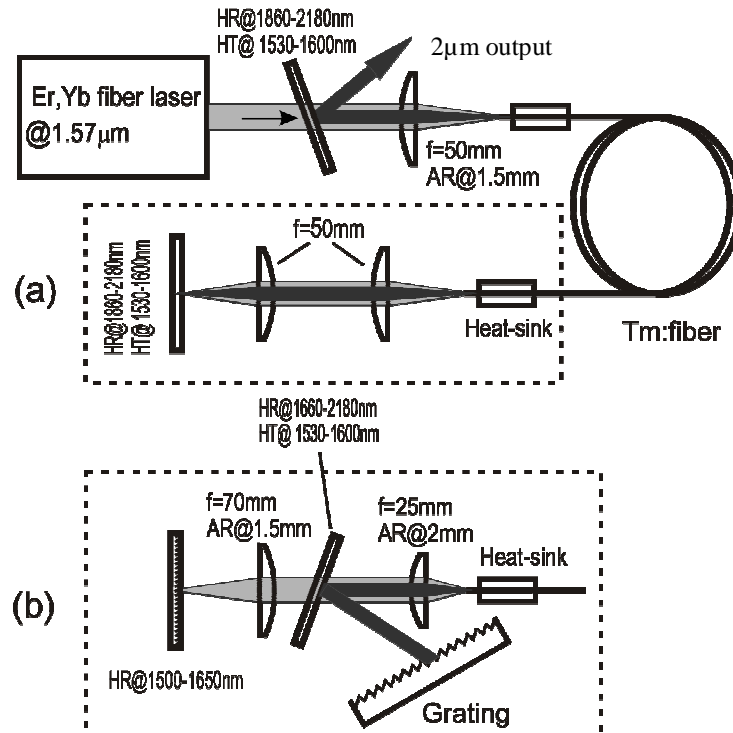


Figure 23: Schematic diagram of Tm fiber laser cladding-pumped by a 1565nm EYDFL (a) free-running operation; (b) tunable operation.

was formed between the perpendicularly-cleaved fiber end-facet at the pump launch end of the fiber (which also served as the output coupler), and, at the opposite end of the fiber, by a simple external cavity comprising a plane dichroic mirror with high reflectivity from 1660nm to 2180nm and high transmission at 1530-1600nm (>92%), and 50mm focal length antireflection coated collimating and focusing lenses. The laser output power characteristics for 8m, 5m and 2.6m fiber lengths are shown in Fig 24. The laser reached threshold at a launched pump power

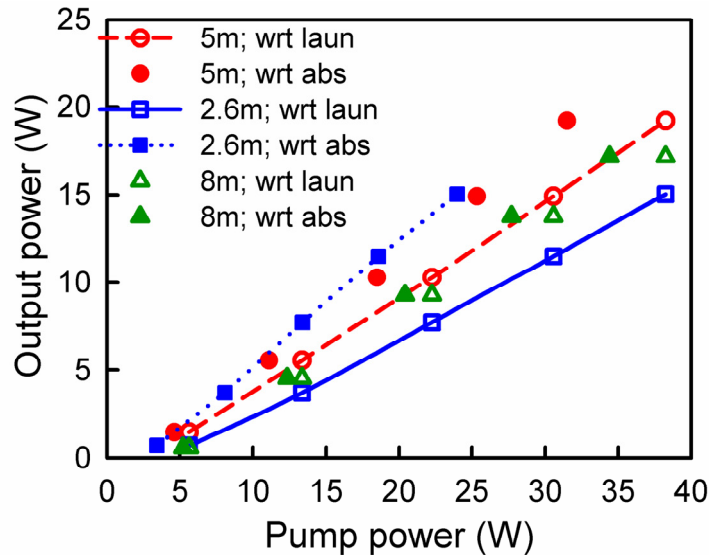


Figure 24: Tm fiber output power versus pump power for 2.6m (square), 5m (circle) and 8m (triangle) fibers. Data plotted in filled and open symbols are with respect to absorbed and launched pump power respectively.

of 3.1W for the 5m fiber and produced an output power of 19.2W at 1991nm for a launched pump power of 38.2W. The unabsorbed 1565nm pump light was measured to ~ 6.7W at the highest pump power of 38.2W and the slope efficiency with respect to the absorbed pump power was ~ 69%. A lower output power of 15W was obtained at 1977nm for the 2.6m fiber due to less pump absorption. The unabsorbed pump power was reached 14W for 38W of launched pump power and the slope efficiency with respect to absorbed pump power was ~72%. This compares favourably with the upper limit of ~79% determined by the Stoke efficiency. Laser performance in terms of maximum output power, slope efficiency, unabsorbed pump power, etc are summarized in Table 2. It can be seen from Fig. 24 for all fiber lengths that there is no evidence of any detrimental thermal effects, suggesting that there is plenty of scope for further power scaling.

Wavelength tuning was achieved by modifying the external cavity design to include an antireflection-coated ($T > 98\%$ at $2\ \mu\text{m}$) Infrasil plano-convex collimating lens of focal length, 25mm, and a simple diffraction grating with 600 lines/mm in the Littrow configuration to provide wavelength selective feedback, as shown in Fig. 23(b). In these experiments a shorter length of fiber (~2.5m) was employed and the unabsorbed pump light after a single-pass was retro-reflected, by an additional plane mirror with high reflectivity at 1500-1650nm and a 70mm

focal length focusing lens with high transmission at $1.5\mu\text{m}$, to improve the pump absorption efficiency. It was estimated that, with this setup, $\sim 65\%$ of the unabsorbed pump power in the first-pass was re-launched into the fiber for a second-pass. The fiber-end nearest the grating was angle-polished at $\sim 8^\circ$ to suppress broadband feedback from the uncoated face that might otherwise compete with the wavelength-dependent feedback provided by the grating and thus

Fiber length (m)	λ (nm)	Slope efficiency (%)		P_{th} (W)	Unabsorbed Power (W)	P_{out} (W)
		wrt P_{launch}	wrt P_{abs}			
2.6	1977	46	72	3.3	14.3	15.0
5	1991	56	69	3.1	6.7	19.2
8	2006	52	58	2.9	3.8	17.2

Table 2: Summary of the laser performance for 2.6m, 5m and 8m fibers cladding-pumped by an Er,Yb fiber laser.

restrict the tuning range. The external cavity in Fig. 23 (b) was first optimized for free-running operation by aligning the $2\mu\text{m}$ plane high reflectivity mirror perpendicular to the collimated beam from the fiber end and retro-reflecting the beam into the fiber. With this two-pass pump absorption scheme, the maximum output power was $\sim 19\text{W}$ for 38.2W of launched pump power. This is comparable to the maximum power generated from the 5m fiber for the laser configuration shown in Fig. 23(a). The corresponding slope efficiency with respect to launched pump power was $\sim 55\%$. Tilting the $2\mu\text{m}$ high reflecting mirror at a small angle ($\sim 10^\circ$) and placing the grating in the beam resulted in a slightly lower maximum power of 17.4W at 1941nm with a corresponding slope efficiency of 50% (see inset of Fig. 25). The threshold pump power

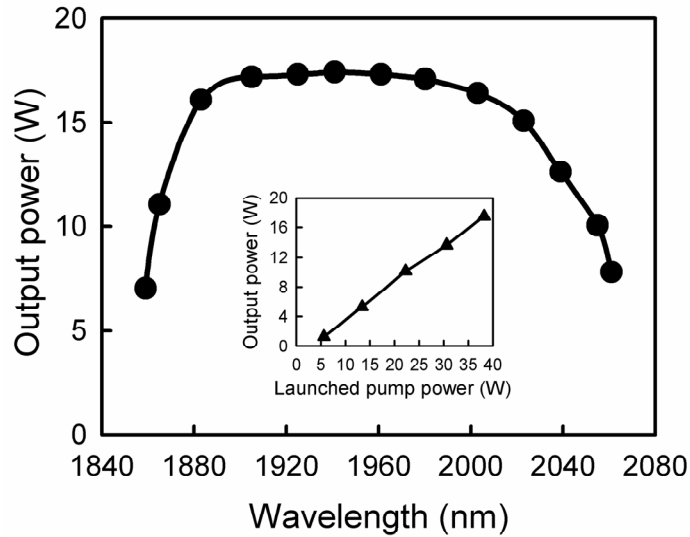


Figure 25: Tunable Tm fiber laser output power versus operating wavelength for 2.6m fiber. Inset: Output power at 1941 nm versus launched pump power.

was $\sim 3\text{W}$ (launched). The lasing wavelength could be tuned over 202nm from 1859 to 2061nm and the output power exceeded 15W over a tuning range of 150nm from ~ 1875 to 2025nm (see Fig. 25). The output linewidth (FWHM) was $<0.5\text{nm}$. The power stability of the laser output was monitored with a high speed InGaAs detector. There was no self-pulsing observed and the short-term stability was measured to be $<0.9\%$ (RMS) on a time scale of 10ms for operating wavelengths $<2010\text{nm}$. The laser became noisier at longer wavelengths, the short-term stability was $\sim 2\%$ at 2025nm and the output signal shown regular pulsing at $\sim 2051\text{nm}$ at a repetition rate of $\sim 3.6\text{kHz}$ with amplitude fluctuations of $\sim 45\%$ (see Fig. 26).

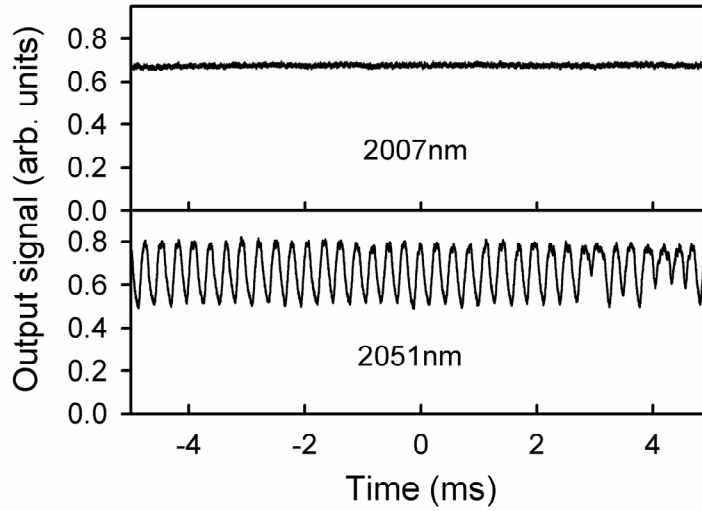


Figure 26: Time evolution of the Tm fiber laser output

There is clearly a great deal of scope for improving the design of the Tm-doped fiber. For example, the inner-cladding diameter could be reduced by over a factor-of-two leading to a much shorter device length, without reducing the pump launch efficiency. In fact, it should be possible to focus the multimode EYDFL to a beam diameter of $<20\mu\text{m}$, so the alignment tolerances for the pump optics and TFL should be very relaxed. This would also allow for pumping with the spatially-multiplexed beams from multiple EYDFLs as one possible route for further power scaling.

4.5 Core pumped Tm fiber laser

We have also investigated core-pumped Tm fiber laser configurations. In this study, a much shorter length of Tm fiber ($\sim 24\text{cm}$) was employed due to the high core-absorption ($\sim 170\text{dB/m}$). Pump light was launched into the core of a 24cm length of fiber (A) using a 25mm focal length lens (see Fig. 27) with high transmission ($>98\%$) at $2\mu\text{m}$ and a transmission of 91% at the pump wavelength of $1.565\mu\text{m}$. Feedback for laser oscillation was provided by the 3.6% Fresnel reflection from the perpendicularly-cleaved fiber end facet at the pump launch end of the fiber (which as served as the output coupler), and, at the opposite end, by a dichroic mirror with high

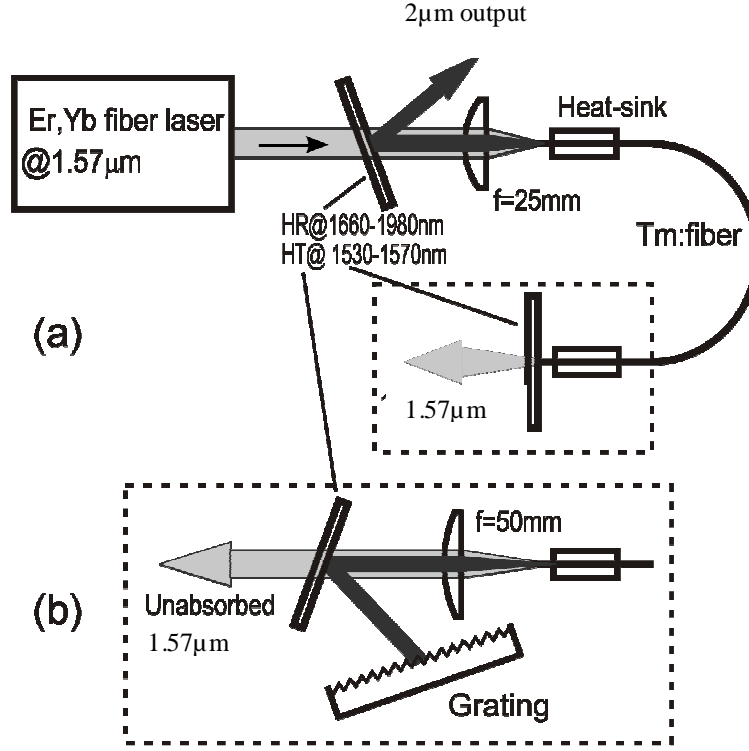


Figure 1: Schematic diagram of the Tm fiber laser core-pumped by an 1565nm Er,Yb fiber laser. ((a) Free-running operation; (b) Tunable operation).

reflectivity at 1660-1980nm (>99.8%) and high transmission at 1530-1570nm (>80%) butted directly to the fiber end. A dichroic mirror with the same coating was used to extract the output from the pump beam at the pump launch end. In view of the very strong pump absorption in the core, the length of bare fiber protruding from the heat-sink at the pump input end was kept very short (<4mm) to minimise the risk of damage. The remainder of the fiber (i.e. with polymer outer coating) was carefully mounted in a water-cooled heat-sink to ensure efficient cooling. The unabsorbed pump power was monitored during the experiments. For the non-tunable cavity configuration as shown in Fig. 27(a), a maximum output power of 12.1W at 1861nm was generated for 23.1W absorbed pump power (see Fig. 28) with corresponding slope efficiency with respect to the absorbed pump power of 58.6%. The threshold pump power (absorbed) was ~ 2.5W. It can be seen from that the laser output power increases in a linear fashion with respect to pump power up to the highest power in spite of the high pump deposition density. This implies that the maximum output power was limited mainly by the available pump power and not by thermal effects. We attribute this to both the low quantum defect heating and the efficient cooling arrangement employed. It is worth noticing that, with the pump launching scheme used in this experiment, only ~ 55% of pump power that is incident on the fiber end facet was coupled directly into the core. The remainder was launched into the inner-cladding, but contributes little to the total absorbed pump power due to the much lower absorption coefficient for cladding pumping.

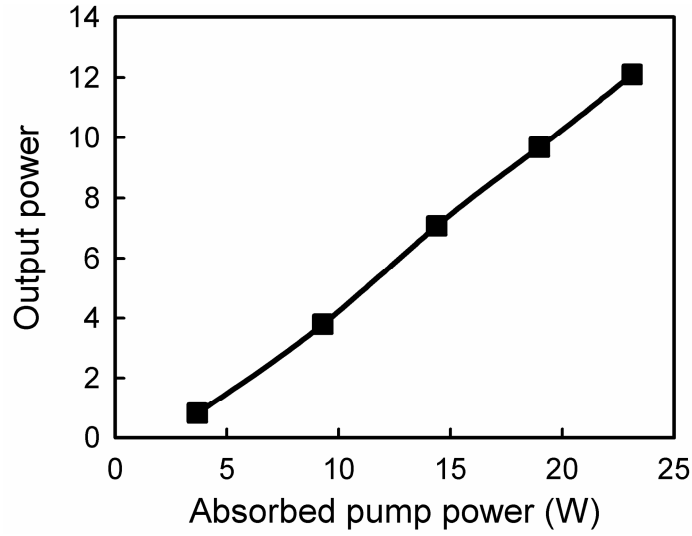


Figure 28: Output power of 24-cm core-pumped Tm fiber laser versus absorbed pump power at 1565 nm.

For the tunable operation, an external cavity configuration was employed, as shown in Fig. 27(b), comprising the same diffraction grating as in cladding-pump Tm fiber laser experiments. A dichroic mirror with high reflectivity ($>99.8\%$) at $1.66\text{-}1.98\mu\text{m}$ and high transmission ($>80\%$) at $1.53\text{-}1.57\mu\text{m}$ was used to separate the $2\mu\text{m}$ signal and the unabsorbed pump light in the external cavity. With this cavity configuration, we obtained up to 8.4W of output at 1827nm with a threshold of 2.7W (absorbed), and a slope efficiency of 46% with respect to absorbed pump power (see inset of Fig. 29). The operating wavelength was tunable over 250 nm from

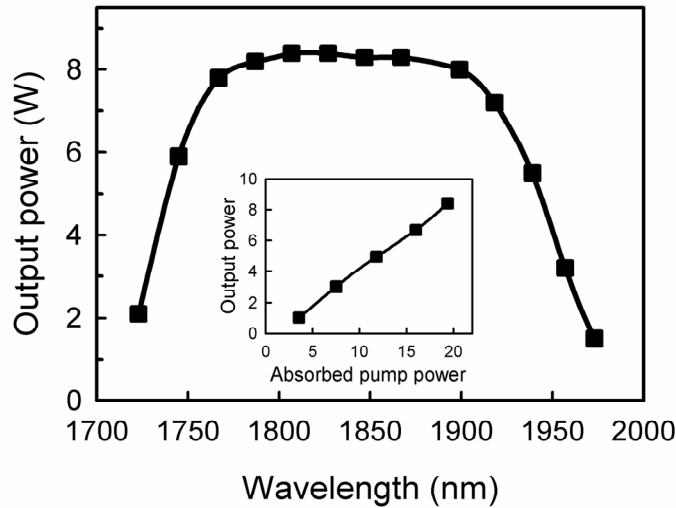


Figure 29: Tunable laser output power versus operating wavelength (Inset: Output power at 1827nm versus absorbed 1565nm pump power).

1723-1973 nm (see Fig. 29). Hence the overall tuning range for core and cladding-pumped laser configurations extends over 338nm from 1723 to 2061nm. To the best of our knowledge this represents the broadest tuning range and shortest operating wavelength achieved from a high-power Tm-doped silica fiber laser reported to date. The output signal was monitored with a high-speed photo-detector during the whole experiment and no self-pulsing was observed over the whole 250nm tuning range at all power levels. The short-term stability was verified to be <1% (RMS) for all operating wavelengths. Further details of this work can be found in Appendix A2 and in the publication [4] listed at the end of this report.

4.6 Q-switched operation of a Tm fiber laser

For many applications it is necessary to operate lasers in a pulsed mode. Pulsed (Q-switched) operation of a core-pumped Tm fiber laser was recently demonstrated using a Nd:YAG laser operating at $\sim 1.3\mu\text{m}$ as the pump source [17,18]. Pulses of peak power, 4.1kW and pulse duration, 150ns were generated. However, Tm fiber lasers pumped at this wavelength band (i.e. $^3\text{H}_6 - ^3\text{H}_5$) are limited to relatively low slope efficiencies. In this section, we described the results of a preliminary study into Q-switched operation of cladding-pumped Tm fiber lasers. In this study we made use of Tm fiber (B) and a two 792nm diode-bar pump sources. The absorption coefficient at 792nm for this fiber is $\sim 6\text{dB/m}$ and so a relatively short length of fiber ($\sim 1.9\text{m}$) was used in our experiments. The two diodes were polarization-combined and the resulting beam was re-formatted with the aid of a two-mirror beam-shaper, to produce a beam with beam propagation factors in orthogonal planes of $M_x^2 \approx 80$ (parallel to the array) and $M_y^2 \approx 52$ (perpendicular to the array) and a maximum power of $\sim 52\text{ W}$ at 790nm. A schematic diagram of the laser configuration used in our experiments is shown in Fig. 30. The laser cavity was formed

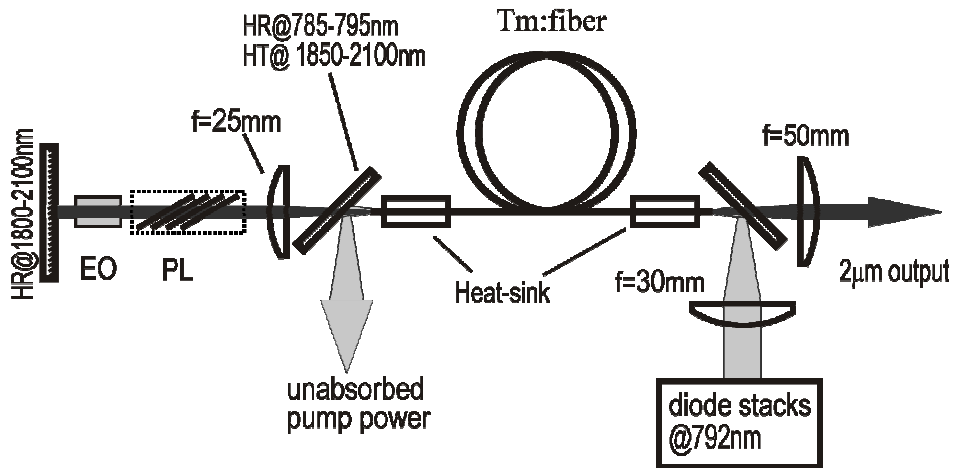


Figure 30: Schematic diagram of the cladding-pumped Tm fiber laser set-up for Q-switched operation. (EO: electro-optic modulator; PL, polarizer).

between the perpendicularly-cleaved fiber end-facet at the pump launch end of the fiber (which also served as the output coupler), and, at the opposite fiber end, by a simple external cavity comprising a plane dichroic mirror with high reflectivity ($>99\%$) from 1800nm to 2100nm and

high transmission the pump wavelength ($T > 97\%$ at 792nm), and a 25 mm focal length

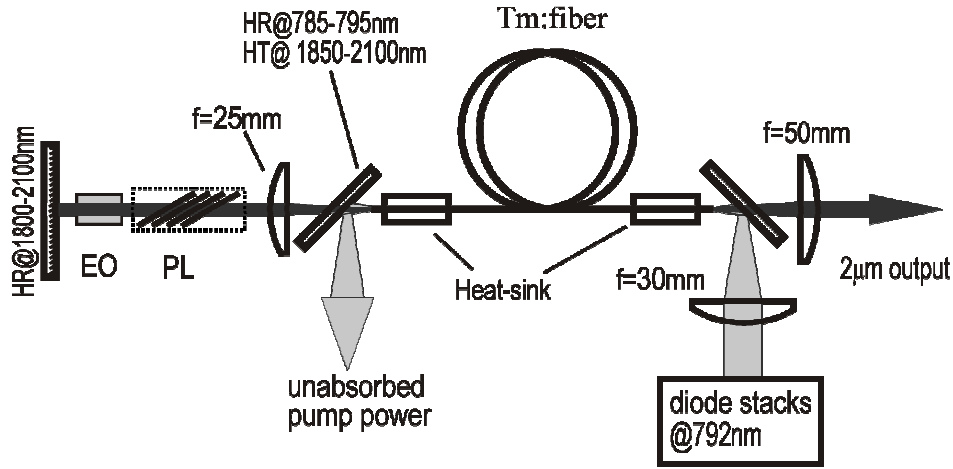


Figure 30: Schematic diagram of the cladding-pumped Tm fiber laser set-up for Q-switched operation. (EO: electro-optic modulator; PL, polarizer).

antireflection coated collimating lens. The fiber-end in the external cavity was angle-polished at $\sim 14^\circ$ to suppress broadband feedback from the uncoated face. The distance between the polished fiber end and the $2\mu\text{m}$ high-reflection mirror was $\sim 27\text{cm}$. Pump light was coupled into the output end of the Tm-doped fiber using a 30mm aspheric focusing lens, and a dichroic mirror with high reflectivity ($>98\%$) at 792nm and high transmission ($>97\%$) at 1800-2100nm at 45° was used to allow extraction of the two-micron fiber laser output. Using this arrangement, the launching efficiency into the fiber was estimated to be $\sim 85\%$. The unabsorbed 792nm pump light was reflected out of the laser resonator with an identical dichroic at the other end of the fiber. Q-switched operation was achieved by incorporating a rubidium titanyl phosphate (RTP) Pockels cell (with a 4mm aperture and a half-wave voltage of 0.7 kV at 632.8nm) and a multi-plate polarizer composed of four ZnSe plates at Brewster's angle. In the experiment, the quarter-wave voltage ($\sim 0.35\text{kV}$) was applied to the Pockels cell (EOM) to prevent optical feedback to the fiber as required for Q-switching. To estimate the impact of the insertion loss induced by the EOM and multi-plate polariser, the output power for CW operation was measured before and after insertion of these optical components. The laser generated an output power of 9.3W for $\sim 24\text{W}$ of launched pump power with corresponding slope efficiency with respect to launched pump power of 49.2% without the EOM and polariser. The laser output power and slope efficiency reduced to 8.5W and 44.9% with the polariser incorporated, and to 8W and 42.8% with both the polariser and EOM inserted into the cavity.

The laser was operated at pulse repetition frequencies (PRF) of 0.7 – 20kHz and stable pulses were generated for a launched pump power of 9.6W. The position and orientation of the polariser and the electro-optic modulator was first carefully optimized to ensure efficient output and to prevent pre-lasing and post-lasing to maximise the output pulse energies. The average output and pulse energy as a function of repetition rate are shown in Fig. 31. Figure 32 shows the dependency of peak power and pulse duration (FWHM) on the repetition rate. An average output of 1.78W was generated for a PRF of 20kHz with a pulse duration of $\sim 200\text{ns}$,

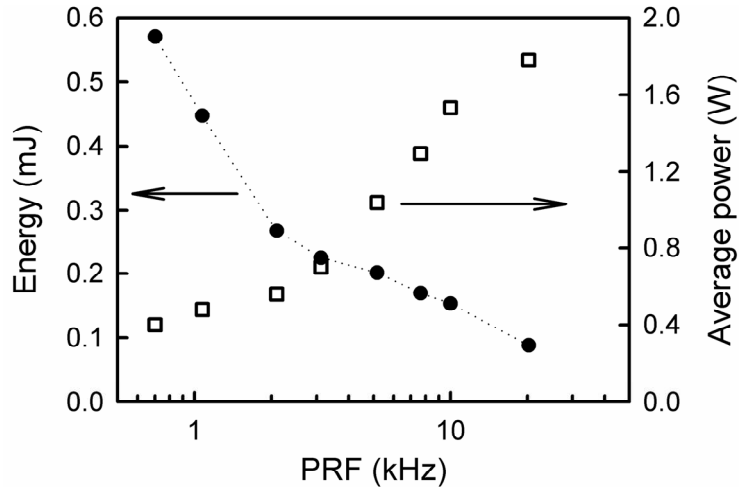


Figure 31: Pulse energy and average power versus repetition rate.

corresponding to a pulse energy of 0.08 mJ and a peak power of 0.4 kW. For a repetition rate of 700 Hz, the average output power was 0.4W and the pulse duration was 110ns, corresponding to a pulse energy of 0.57mJ and a peak power of ~5.2kW. It was found that high cleaving quality of the fiber end is very important in Q-switched operation, otherwise the fiber end was susceptible to damage due to the high intensity. Tunable Q-switched operation was demonstrated by replacing the 2 μ m high reflectivity mirror (Fig. 30) with a simple diffraction

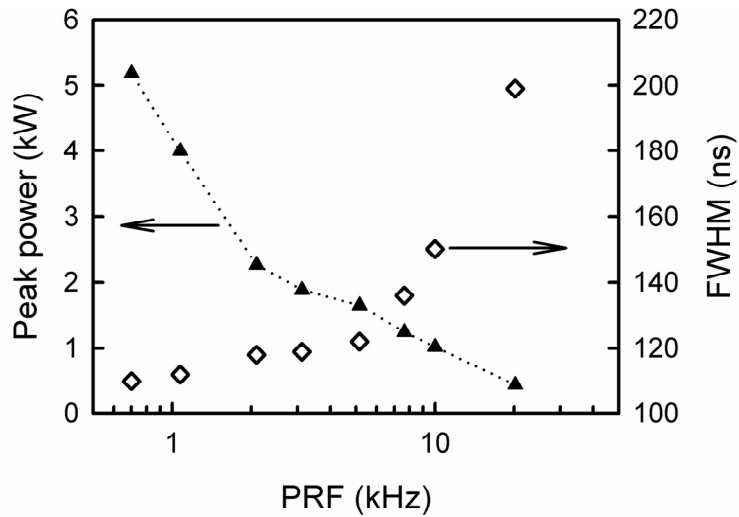


Figure 32: Peak power and pulse duration versus pulse repetition frequency.

grating (as described in section 4.4) with 600 lines/mm in the Littrow configuration to provide wavelength selective feedback. For a launched pump power of ~7W, the laser generated an average output of 280mW at 0.7 kHz PRF with a pulse duration of 120ns. The corresponding pulse energy and peak power were 0.41mJ and 3.4kW respectively. The operating wavelength

was tunable over a range of 154nm from 1935nm to 2089nm. The use of higher pump power and/or lower PRF's would in principle yield higher pulse energies, but may be limited by onset of pre-lasing, post-lasing and amplified spontaneous emission (ASE). Further scaling in output pulse energy would require further optimization of both the Tm fiber design and laser resonator design.

4.7 Summary and future prospects

We have demonstrated efficient operation of Tm fiber lasers in both cladding-pumped and core-pumped laser configurations in-band pumped by an Er,Yb fiber at 1565nm. We have also presented the results of a preliminary study aimed at improving the efficiency of Tm fiber lasers pumped at 0.8 μ m. The results presented in this report demonstrate two main advantages of in-band pumping over other pumping schemes. The first is that very high lasing efficiencies can be achieved and, as a result of the low quantum defect heating, it should be possible to scale to much higher power levels. The second advantage of this approach is that there is a great deal of flexibility in the fiber design and the operating wavelength. The latter is mainly due to the relatively good beam quality for Er,Yb fiber sources, which allows the use of core-pumped (or close-area-ratio cladding-pumped) fiber configurations. In this preliminary study we have obtained output powers up to 19.2W at 1991nm from a cladding-pumped laser configuration for ~38.2W of launched pump power at 1565nm and slope efficiencies with respect to absorbed pump power up to 72%. Slightly lower efficiencies for longer fibers indicate the inner-cladding guide loss for the pump and/or the core propagation loss for laser light have detrimental impact on performance. Thus, further work on the Tm fiber design to reduce cladding/core loss is needed. One way to remedy this problem would be to use a fiber design with a smaller inner-cladding-to-core area ratio, since this would allow the use of shorter fiber lengths with lower loss. For core-pumped laser configurations, very short fiber lengths can be employed. In a simple demonstration of a core-pumped device with a 24cm long fiber, we obtained up to 12.1W of output at 1851nm for 23.1W absorbed pump power. Wavelength tuning was realized by use of an external cavity containing a diffraction grating. The operating wavelength could be tuned over 250nm from 1723nm to 1973nm. The combined wavelength tuning range for core and cladding pumped Tm fiber lasers extends from 1723nm to 2061nm. This is an extremely broad tuning range and will almost certainly benefit a range of applications. In contrast, direct diode pumping at ~790nm offers higher overall efficiencies, but, due to the poor beam quality of high power diode sources, offers rather limited flexibility in fiber design and in operating wavelength. By optimising the fiber design to exploit the efficiency enhancing 'two-for-one' cross-relaxation process, we have demonstrated slope efficiencies with respect to absorbed power up to 65%. We have also demonstrated a Q-switched fiber laser, based on the same fiber, with pulse energies ~0.6mJ and peak powers >5kW. Further increase in pulse energy and peak power should be possible by further optimising the fiber design and by pumping at 1565nm.

5.0 CONCLUSIONS AND FUTURE WORK

In-band pumping of a Tm fiber laser by a cladding-pumped Er,Yb fiber laser has been investigated. Preliminary results indicate that this 'fiber-fiber' hybrid laser scheme is a

promising approach for generating high-power/high-pulse-energy and widely tunable output in the 2 μ m spectral region with high operation efficiency and good beam quality. For further power scaling, however, it is going to be necessary to improve the design of the Tm-doped fiber. More specifically, the inner-cladding-to-core area ratio should be reduced to increase the pump absorption coefficient for cladding-pumped configurations to allow much shorter device lengths. This should allow scaling of Tm fiber laser output power to well beyond 100W with slope efficiency >70% using single or multiple high power Er,Yb fiber pump sources. Further extension of the range of operating wavelengths may also be possible by tailoring the Tm fiber design for operation in the desired wavelength regime and by employing in-fiber Bragg gratings for wavelength selection.

6.0 REFERENCES

1. R. A. Hayward, W. A. Clarkson, P. W. Turner, J. Nilsson, A. B. Grudinin and D. C. Hanna, "efficient cladding-pumped Tm-doped silica fiber laser with high power single mode output at 2 μ m" *Electron. Lett.*, vol.36, pp.711-712 (2000).
2. W. A. Clarkson, N. P. Barnes, P. W. Turner, J. Nilsson and D. C. Hanna, "High-power cladding-pumped Tm-doped silica fiber laser with wavelength tuning from 1860 to 2090 nm" *Opt. Lett.*, **27**, pp.1989-1991 (2002).
3. M. Laroche, P. Jander, W.A. Clarkson, J.K. Sahu, J. Nilsson and Y. Jeong, "High power cladding-pumped tunable Er,Yb-doped fibre laser," *Electron. Lett.* **40**, 855-856 (2004).
4. J. Jeong, C. Alegria, J.K. Sahu, L. Fu, M. Ibsen, C. Codemard, M.R. Mokhtar, and J. Nilsson, "A 43-W C-band tunable narrow-linewidth Erbium-ytterbium co-doped large-core fiber laser," *IEEE Photon. Technol. Lett.* **16**, 756-758 (2004).
5. J.E. Townsend, W.L. Barnes, K.P. Jedrzejewski and S.G. Grubb, "Yb³⁺ sensitised Er³⁺-doped optical fibre in silica host with very high transfer efficiency," *Electron. Lett.*, **27**, pp.1958-1959, (1991).
6. J. Nilsson, S.-U. Alam, J.A. Alvarez-Chavez, P.W. Turner, W.A. Clarkson, and A.B. Grudinin, "High-power and Tunable operation of Erbium-ytterbium co-doped cladding-pumped fibre lasers," *IEEE J. Quantum Electron.* **39**, 987-994 (2003).
7. J.K. Sahu, Y. Jeong, D.J. Richardson and J. Nilsson, "A 103 W erbium-ytterbium co-doped large-core fiber laser," *Opt. Comm.* **227**, 159-163 (2003).
8. G. G. Vienne, J.E. Caplen, L. Dong, J. D. Minelly, J. Nilsson, and D.N. Payne, "Fabrication and characterization of Yb³⁺:Er³⁺ phospho-silicate fibers for lasers," *J. Lightwave Technol.* **16**, pp. 1990-2001, (1998).
9. D. C. Brown and H. J. Hoffman, "Thermal, stress and thermo-optic effects in high average power double-clad silica fiber lasers," *J. Quantum Electron.*, **37**, pp.207-217 (2001).
10. D.C. Hanna, I.R. Perry, J.R. Lincoln, "A 1-Watt thulium-doped cw fibre laser operating at 2 μ m," *Opt. Comm.* **80**, pp.52-26 (1990).
11. P.S. Golding, S.D. Jackson, P.K. Tsai, B.C. Dickinson, T.A. King, "Efficient high power operation of a Tm-doped silica fiber laser pumped at 1.319 μ m" *Opt. Comm.* **175**, pp.179-183 (2000).
12. Y.H. Tsang, D.J. Coleman, T.A. King, "High power 1.9 μ m Tm³⁺-silica fibre laser pumped at 1.09 μ m by a Yb³⁺-silica fibre laser," *Opt. Comm.* **231**, pp.357-364 (2004).

13. Y. Jeong, P. Dupriez, J. K. Sahu, J. Nilsson, D.Y. Shen, W. A. Clarkson, S. D. Jackson, "Power scaling of 2 μ m ytterbium-sensitized thulium-doped silica fibre laser diode-pumped at 975 nm," *Electron. Lett.*, **41**, pp.173-174, (2005).
14. S. D. Jackson and S. Mossman, "Efficiency dependence on the Tm³⁺ and Al³⁺ concentrations for Tm³⁺-doped silica double-clad fiber laser," *Appl. Opt.*, **42**, pp.2702-2707 (2003).
15. T. Yamamoto, Y. Miyajima and T. Komukai, "1.9 μ m Tm-doped silica fibre laser pumped at 1.5 μ m", *Electron. Lett.*, **30**, pp.220-221, (1994).
16. R.M. Percival, D. Szebesta, C.P. Seltzer, S.D. Perrin, S.T. Davey and M. Louka, "A 1.6- μ m pumped 1.9- μ m thulium-doped fluoride fiber laser and amplifier of very high efficiency," *IEEE J. Quantum Electron.* **31**, pp.489-493 (1995).
17. A.F. El-Sherif, T.A. King, "High-energy, high brightness Q-switched Tm³⁺-doped fiber laser using an electro-optic modulator," *Opt. Comm.* **218**, pp.337-344 (2003).
18. A.F. El-Sherif, T.A. King, "High-peak-power operation of a Q-switched Tm³⁺-doped silica fiber laser operating near 2 μ m," *Opt Lett.* **28**, pp.22-24 (2003).

7.0 PUBLICATIONS

1. D.Y.Shen, J.K.Sahu, W.A.Clarkson, "Highly efficient Er Yb-doped fiber laser with 188W free-running and > 100W tunable output power," *Optics Express* 2005 Vol.13(13) pp.4916-4921.
2. W.A.Clarkson, D.Y.Shen, P.Wang, L.Cooper, J.Nilsson, J.K.Sahu, "High-power fiber lasers: recent developments and future prospects," *Optics and Optoelectronics Conference Warsaw* 30 Aug - 1 Sep 2005 5958-26 (Invited).
3. D.Y.Shen, J.K.Sahu, W.A.Clarkson, "Highly efficient Erbium-Ytterbium co-doped fiber laser with 188W output power at 1565nm," *CLEO/Europe-EQEC 2005 Munich* 12-17 Jun 2005 CJ1-3.
4. D.Y.Shen, V.Shcheslavskiy, J.K.Sahu, W.A.Clarkson, "High-power widely tunable Tm fibre lasers in cladding-pumped and core-pumped cavity configurations," *CLEO/Europe-EQEC 2005 Munich* 12-17 Jun 2005 CJ5.
5. D.Y.Shen, J.I.Mackenzie, J.K.Sahu, W.A.Clarkson, S.D.Jackson, "High-power and ultra-efficient operation of a Tm³⁺-doped silica fiber laser," *ASSP 2005 Vienna* 6-9 Feb 2005 MC6.
6. D.Y. Shen, V.Shcheslavskiy, J.K.Sahu, W.A.Clarkson, "High-power widely tunable Tm:fibre lasers pumped by an Er,Yb co-doped fibre laser," to be submitted.
7. Y.Jeong, P.Dupriez, J.K.Sahu, J.Nilsson, D.Y.Shen, W.A.Clarkson, S.D.Jackson, "Power-scaling of a 2 micron ytterbium-sensitized thulium-doped silica fibre laser diode-pumped at 975nm," *Electronics Letters* 2005 Vol.41(4) pp.173-174.

8. Y.Jeong, P.Dupriez, J.K.Sahu, J.Nilsson, D.Shen, W.A.Clarkson, S.D.Jackson,
“Thulium-ytterbium co-doped fiber laser with 75W of output power at 2 microns,” *SPIE European Symposium on Optics and Photonics for Defence & Security* London 25-28 Oct 2004 Paper 5620-4.
9. Y.Jeong, P.Dupriez, J.K.Sahu, J.Nilsson, D.Shen, W.A.Clarkson, S.D.Jackson,
“Thulium-ytterbium co-doped fiber laser with 32W of output power in the 2 micron wavelength range,” *EPS-QEOD Europhoton* Lausanne 29 Aug - 3 Sep 2004 TuB3

Appendix A1

Highly efficient Er,Yb-doped fiber laser with 188W free-running and > 100W tunable output power

D. Y. Shen, J. K. Sahu and W. A. Clarkson

Optoelectronics Research Centre, University of Southampton, Southampton SO17 1BJ, United Kingdom
des@orc.soton.ac.uk

Abstract: Efficient high-power operation of an erbium-ytterbium co-doped fiber laser cladding-pumped by two spatially-multiplexed and polarization combined 975 nm diode-stacks is reported. Up to 188 W of continuous-wave output at 1.57 μm was generated with a beam-quality factor (M^2) of 1.9 and an overall slope efficiency with respect to launched pump power of 41% (and 43% for output powers <120W). Tunable operation was demonstrated by use of an external cavity containing a diffraction grating and a maximum output power of 108 W at 1538 nm was generated for a launched pump power of ~ 336 W. The operating wavelength was tunable from 1531 to 1571 nm, with >100W output power over a tuning range of 36 nm from 1532 nm to 1568 nm.

©2005 Optical Society of America

OCIS code: (140.0140) Lasers and laser optics; (140.3070) Infrared and far-infrared lasers; (140.3480) Lasers, diode-pumped; (140.3510) Lasers, fiber.

References and links

1. A. Levoshkin, A. Petrov and J. E. Montagne, "High-efficiency diode-pumped Q-switched Yb:Er:glass laser," *Opt. Commun.* **185**, 399-405 (2000).
2. J. Nilsson, S.-U. Alam, J.A. Alvarez-Chavez, P.W. Turner, A.A. Clarkson, and A.B. Grudinin, "High-power and Tunable operation of Erbium-ytterbium co-doped cladding-pumped fibre lasers," *IEEE J. Quantum Electron.* **39**, 987-994 (2003).
3. D.C. Brown, and H.J. Hoffman, "Thermal, Stress, and Thermo-Optic Effects in High Average Power Double-Clad Silica Fiber Lasers," *IEEE J. Quantum Electron.* **37**, 207-217 (2001).
4. J.K. Sahu, Y. Jeong, D.J. Richardson and J. Nilsson, "A 103 W erbium-ytterbium co-doped large-core fiber laser," *Opt. Commun.* **227**, 159-163 (2003).
5. M. Laroche, P. Jander, W.A. Clarkson, J.K. Sahu, J. Nilsson and Y. Jeong, "High power cladding-pumped tunable Er,Yb-doped fibre laser," *Electron. Lett.* **40**, 855-856 (2004).
6. J. Jeong, C. Alegria, J.K. Sahu, L. Fu, M. Ibsen, C. Codemard, M.R. Mokhtar, and J. Nilsson, "A 43-W C-band tunable narrow-linewidth Erbium-ytterbium co-doped large-core fiber laser," *IEEE Photon. Technol. Lett.* **16**, 756-758 (2004).
7. G. G. Vieme, J.E. Caplen, L. Dong, J. D. Minelly, J. Nilsson, and D.N. Payne, "Fabrication and characterization of Yb³⁺-Er³⁺ phosphosilicate fibers for lasers," *J. Lightwave Technol.* **16**, 1990-2001 (1998).

1. Introduction

High-power solid-state laser sources operating in the eyesafe wavelength regime around ~ 1.5 - $1.6 \mu\text{m}$ have numerous applications in areas such as remote sensing, range finding, and free space and satellite communications. The traditional approach for producing laser output in this wavelength region is via direct diode pumping of erbium-ytterbium co-doped bulk glass or crystal lasers [1]. Power scaling of such lasers has proved rather difficult due to the high thermal loading density which results from a large quantum defect and the need for relatively high active ion concentrations. The situation is further exacerbated by energy-transfer-upconversion which leads to increased heat generation. For many of these applications, the

#7668 - \$15.00 USD
(C) 2005 OSA

Received 1 June 2005; revised 10 June 2005; accepted 12 June 2005
27 June 2005 / Vol. 13, No. 13 / OPTICS EXPRESS 4916

requirement for high output power is also accompanied by the need of high efficiency and good beam quality, which are often difficult to achieve in conventional 'bulk' Er-doped solid-state laser owing to high thermal loading. Moreover, the combination of relatively narrow emission linewidths and rather low gains that are typical in conventional solid-state lasers restricts the range of operating wavelengths and hence further limits their applicability. Cladding-pumping of Er,Yb-doped fiber lasers (EYDFLs) offers a promising route to output in this spectral region [2] with the attraction of a geometry that has a high degree of immunity from the effects of thermal loading, and allows scaling to high power levels without decreasing efficiency or degrading beam quality [3]. Moreover, the broad emission linewidths that are typical in glass hosts allows for flexibility in the operating wavelength. To date, operation of an EYDFL with 103 W of continuous-wave output power at 1.57 μm has been reported for free-running cavity configuration (i.e. with no wavelength selection) with a slope efficiency of 30% with respect to launched pump power [4]. Tunable operation of an EYDFL has been reported with output powers up to 30 W [5] and 43 W [6] cladding-pumped by 940 nm and 975 nm diode lasers respectively. In this paper we report a highly efficient $\text{Er}^{3+}\text{-Yb}^{3+}$ co-doped fibre laser, cladding pumped by a 975 nm diode-stack source, that generates up to 188 W of continuous-wave (cw) output at 1565 nm with an overall slope efficiency of 41% with respect to launched pump power. We have also demonstrated tunable operation by use of an external cavity containing a diffraction grating achieving a maximum output power of 108 W at 1538 nm for a launched pump power of ~ 336 W. The operating wavelength could be tuned over 36 nm from 1532 to 1568 nm at output power levels >100 W and with a linewidth of ~ 1 nm.

2. Experiments and results

The double-clad Er,Yb co-doped fibre (EYDF) used in our experiments was pulled from a preform fabricated in-house using the standard modified chemical vapour deposition (MCVD) and the solution doping technique [7]. The fibre had an Er,Yb-doped phospho-silicate core of 30 μm diameter and 0.22 NA, surrounded by a pure silica D-shaped inner-cladding of 400 μm diameter (~ 360 μm along the short axis). The latter was coated with a low refractive index ($n=1.375$) UV curable polymer outer-cladding to produce a high numerical aperture (~ 0.4 NA) waveguide for the pump and hence to facilitate efficient launch of pump light from high-power (but low-brightness) diode sources. Pump power was provided by two 975 nm diode-stacks which were spatially-combined by inter-leaving their output beams using a slotted-mirror beam-combiner. The resulting beam was then slit into two beams which were subsequently polarization-combined to produce a single beam of relatively high-brightness with beam propagation factors of $M_x^2 \sim 150$ (in the stacking direction) and $M_y^2 \sim 200$ (in the orthogonal direction), and with a maximum power of ~ 700 W. The resulting beam was then split into two beams of roughly equal power and with $M_x^2 \sim 150$ and $M_y^2 \sim 100$ allowing pumping of the EYDFL from both ends, as shown in Fig. 1(a). Pump light was launched into opposite ends of the fiber with the aid of anti-reflection coated lenses of 25 mm focal length and dichroic mirrors with high reflectivity ($>99.5\%$ at 45°) at the pump wavelength, and high transmission ($>98\%$) at 1530-1570 nm to allow efficient extraction of the EYDFL output. With this pump arrangement, the launch efficiency into the fiber was estimated to be $\sim 80\%$. The effective absorption coefficient for the fiber for pump light centered 975 nm was measured to be $\sim 6.9\text{dB/m}$, and hence a relatively short fiber length of ~ 3 m was selected for the free-running EYDFL. The combination of this short device length and the relatively large core diameter of 30 μm are important for preventing self-pulsing and avoiding detrimental nonlinear process that would otherwise lead to a roll-over in output power or damage at the fiber end facets. Both end sections of the fiber were carefully mounted in water-cooled V-groove heat sinks to prevent thermal damage to the fiber coating due to unlaunched pump power and by heat generated in the core due to quantum defect heating. Feedback for laser

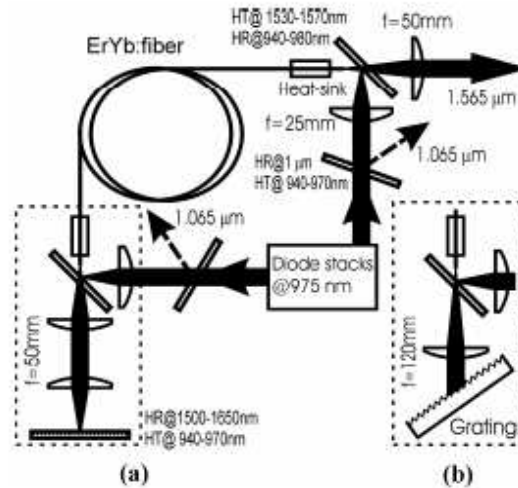


Fig. 1. Schematic diagram of cladding pumped Er,Yb fiber laser: (a) free-running configuration; (b) external cavity of the tunable fibre laser.

oscillation was provided by the 3.6% Fresnel reflection from a perpendicularly-cleaved fiber end facet, at one end of the fibre, and, at the opposite end, by a simple external cavity comprising a plane mirror with high reflectivity ($>99.5\%$) at $1.5\text{--}1.65\text{ }\mu\text{m}$ and high transmission ($>95\%$) at $940\text{--}970\text{ nm}$, and anti-reflection coated 50 mm focal length collimating and focusing lenses.

Dichroic mirrors with high reflectivity at $1\text{ }\mu\text{m}$ and high transmission at 975 nm were inserted into the two pump arms to prevent any $\sim 1\text{-}\mu\text{m}$ radiation, due to parasitic lasing on the Yb^{3+} transition, from being fed back to the diode-stacks. The laser output was collimated with a 50 mm focal length lens with high transmission at $1.5\text{--}1.65\text{ }\mu\text{m}$. Using this arrangement the laser reached threshold at a combined incident pump power of $\sim 3\text{ W}$ and generated a maximum output power of 159 W at 1565 nm with a linewidth of $\sim 2.6\text{ nm}$ (FWHM) for a total incident pump power of 582 W (466 W launched), corresponding to an average slope efficiency (with respect to launched power) of 34.1% (see Fig. 2). The laser had a higher slope

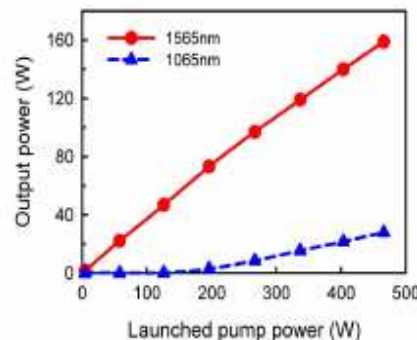


Fig. 2. Output power versus launched pump power for free-running Er,Yb fiber laser with an external cavity.

efficiency of 37.3% at low pump powers (<220 W) which decreased to 31.2% at high pump power due to the onset of parasitic lasing on the Yb^{3+} transition at $\sim 1\mu\text{m}$. The feedback for $1\mu\text{m}$ lasing was provided by the two perpendicularly-cleaved fiber end facets and the combined output at $1.065\mu\text{m}$ was measured to be <28 W. The beam quality factor (M^2) for the EYDFL was measured to be 1.9, which was a little better than expected given that the core has a V value of ~ 13 . The power stability of the laser output was monitored with a high speed InGaAs detector (bandwidth of 50 MHz) and a 100 MHz digital oscilloscope and no self-pulsing was observed at all power levels. Removing the high reflectivity mirror from the external cavity, so that feedback for both $1\mu\text{m}$ and $1.57\mu\text{m}$ lasing was provided by the two perpendicularly-cleaved fiber end facets, resulted in a combined output power of 188 W at 1565 nm for a launched pump power of 466 W (see Fig. 3). The overall slope efficiency with respect to

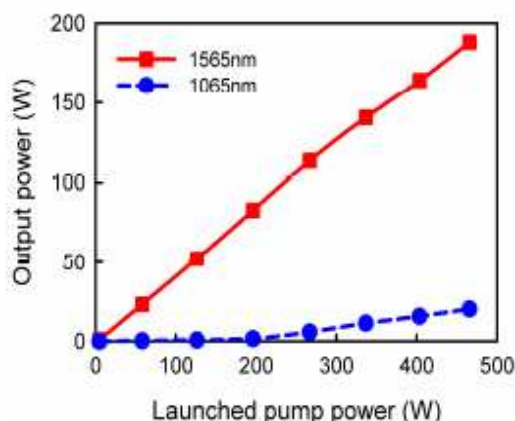


Fig. 3. Output power versus launched pump power with no external cavity.

launched pump power was 41%. Similarly, the laser exhibited a high slope efficiency of 43.1% at low pump powers (<300 W), which decreased to 36.8% at high pump powers due once again to lasing on Yb^{3+} transition. In this case, lasing at 1065 nm resulted in a total output power (i.e. from both fiber ends) of <20 W. It is interesting to note that the $1\mu\text{m}$ power was significantly lower for the latter cavity configuration. This is believed to be due to lower cavity losses at $1\mu\text{m}$ for the former cavity configuration (shown in Fig.1(a)) due to residual feedback from the external feedback cavity at $\sim 1\mu\text{m}$. One way to avoid parasitic lasing at $\sim 1\mu\text{m}$ is to increase the cavity loss at $\sim 1\mu\text{m}$ by using an angle cleaved fiber end facet nearest the external cavity and by using a plane mirror with high transmission in the $1030\text{--}1100\text{ nm}$ regime. It is worth noting that the laser output power in Fig. 2 and Fig. 3 is still essentially linear with respect to pump power at even the high pump power if parasitic lasing at $\sim 1\mu\text{m}$ is taken into account, with no evidence of any detrimental impact due to thermal loading. Hence, with the appropriate cavity design and with the required degree of suppression of $1\mu\text{m}$ lasing, it should be possible to obtain a further increase in output power by simply increasing the pump power.

Tunable operation of EYDFL was demonstrated employing a simple external cavity design, as shown in Fig. 1(b), comprising an antireflection coated collimating lens of focal length 120 mm and a simple replica diffraction grating (600 lines/mm) mounted on a copper substrate to facilitate removal of waste heat. A relatively long focal length collimating lens in the external feedback cavity was selected to avoid any possible damage to the grating and to reduce the collimated beam divergence and hence increase the spectral selectivity of the

grating feedback cavity. The grating was blazed for wavelength of $\sim 1.65 \mu\text{m}$ with reflectivity of $\sim 75\%$ for light polarised parallel to the grooves and $\sim 95\%$ for light polarised in the orthogonal direction, and was aligned in the Littrow configuration to provide wavelength selective feedback and hence the means for adjusting the lasing wavelength. The fiber end facet nearest the grating was angle-polished at $\sim 14^\circ$ to suppress parasitic lasing between the two fiber end facets. A shorter fibre length of $\sim 2 \text{ m}$ was selected for the tunable operation and the combined unabsorbed pump power (from two ends) was measured to $< 7 \text{ W}$ for a total launched pump power of 336 W . Using this resonator configuration, the laser generated a maximum output power of 108 W at 1538 nm for $\sim 336 \text{ W}$ of launched pump power (see inset of Fig. 4). The threshold pump power (launched) was $\sim 3.3 \text{ W}$ and the slope efficiency with respect to launched pump power was 32% . The linear dependence of the output power on the pump power suggests that there was no severe thermal induced deformation on the bulk grating even at highest pump power, and clearly indicates that there is scope for further power scaling of this simple tunable EYDFL laser architecture by increasing the pump power. The laser output power as a function of operating wavelength is shown in Fig. 4. The lasing wavelength could be tuned from 1531 to 1571 nm , and over 36 nm from ~ 1532 to 1568 nm at output power levels in excess of 100 W with a linewidth (FWHM) of $\sim 1 \text{ nm}$. The short-term stability was measured to be $< 0.9\%$ (RMS) on a time scale of $300 \mu\text{s}$. Moreover, the output power was very stable over longer time periods with power fluctuations of $< 3\%$ over a time scale of 30 minutes, and we did not observe any degradation in performance over a period of several months of intermittent use.

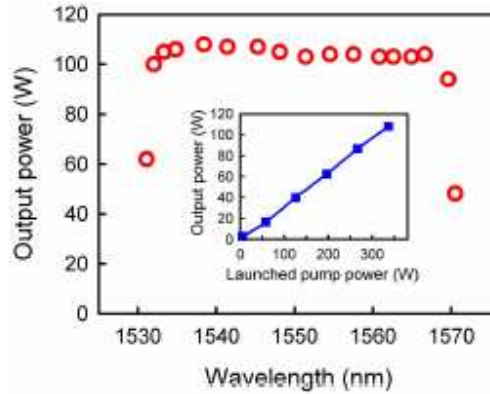


Fig. 4. Tunable Er,Yb fiber laser output power versus operating wavelength for a 2 m fiber. Inset: Output power of the tunable Er,Yb fiber laser at 1538 nm versus launched pump power.

3. Conclusion

In conclusion, efficient and high-power operation of an erbium-ytterbium co-doped fiber laser cladding-pumped by two 975 nm diode-stacks is reported. Up to 188 W of continuous-wave output at $1.57 \mu\text{m}$ was generated with a beam-quality factor (M^2) of 1.9 and an overall slope efficiency with respect to launched pump power of 41% and 43% for low powers ($> 300 \text{ W}$). Tunable operation was demonstrated by use of an external cavity containing a diffraction grating and a maximum output power of 108 W at 1538 nm was generated for a launched pump power of $\sim 336 \text{ W}$. The operating wavelength was tunable from over 36 nm from 1532 nm to 1568 nm at output power levels in excess of 100 W with a linewidth (FWHM) of $\sim 1 \text{ nm}$. The short-term stability was measured to be $< 0.9\%$ (RMS) and the output power was very stable over longer time periods with power fluctuations of $< 3\%$ over a time scale of 30 minutes with no evidence of self-pulsing at any power level. The linearity of output power as

a function of pump power for both the free-running and tunable cavity configurations suggests that there is considerable scope for further power scaling.

Acknowledgments

This work was funded by EOARD under contract numbers F61775-01-C0008 and FA8655-03-1-3057, and by the Engineering and Physical Sciences Research Council (UK).

Appendix A2

High-power widely tunable Tm fibre lasers in cladding-pumped and core-pumped cavity configurations

D. Y. Shen, V. Shcheslavskiy, J.K. Sahu and W. A. Clarkson

Optoelectronics Research Centre, University of Southampton, SO17 1BJ, United Kingdom

Cladding-pumped Tm-doped fibre lasers operating in eye-safe 2- μm spectral region have attracted growing interest in recent years owing to their numerous applications in areas such as lidar and medicine. In contrast to conventional 'bulk' solid-state lasers, fibre-based sources benefit from a geometry that allows relatively simple thermal management and hence offer the prospect of higher output power and improved beam quality. A particular attraction of Tm-doped fibre lasers is the very broad transition linewidth offering the prospect of wide tunability over the ~1700-2100 nm regime. Direct pumping of double-clad Tm-doped silica fibre lasers with diode lasers at ~790 nm [1] and, more recently, Tm-doped silica fibre lasers sensitized by co-doping with Yb at 975 nm [2] has been demonstrated with output powers up to 30 W (limited by available pump power) and 75 W (limited by fibre damage) respectively. In the latter, the slope efficiency was rather low (~26%), due, in part, to the relatively high quantum defect heating (~51%), hence suggesting that power scaling may prove rather difficult via this scheme. An alternative, and more promising, approach for power scaling of Tm fibre lasers is to pump directly into the upper level manifold with an Er fibre laser at 1.55-1.62 μm . This has the attraction of a very high Stokes efficiency (~0.75-0.85) and hence low quantum defect heating, opening up the prospect of very high lasing efficiencies. In addition, the good beam quality available from high-power Er-doped fibre lasers allows direct pumping into the Tm-doped fibre core leading to the possibility of much shorter device lengths. This is critically important for extending the tuning range of Tm fibre lasers to shorter wavelengths. In this paper we report highly efficient operation of Tm-doped silica fibre lasers, pumped by a high-power cladding-pumped Er,Yb fibre laser at 1565nm, in both cladding-pumped and core-pumped resonator configurations. In the cladding-pumped Tm fibre laser we obtained up to 19 W of output at 1991 nm with a slope efficiency of 69% with respect to absorbed pump power, and in the core-pumped laser we obtained a maximum output power of 12.1W at 1860nm limited by available pump power. Using tunable cavity configurations the cladding-pumped and core-pumped Tm fibre lasers could be tuned from 1861 to 2061nm and from 1725 to 1973nm at multi-watt power levels respectively. To the best of our knowledge this represents the broadest tuning range and shortest operating wavelength from a high-power Tm-doped fibre laser reported to date.

The Tm fibre used in our experiments had a Tm-doped alumino-silicate core of 20 μm diameter and 0.12 NA, surrounded by a pure silica D-shaped inner-cladding of 200 μm diameter and 0.49 NA (calculated), with a low refractive index polymer outer-cladding. The pump source was an Er-Yb co-doped fibre laser cladding pumped by a high power diode-stack at 975 nm, which provided up to 58W of output at 1565nm in a beam with $M^2=1.9$. The effective absorption coefficient in the Tm-doped fibre (i.e. for cladding-pumping) at this pump wavelength was measured to be ~1.5 dB/m, and hence a fibre length of ~5 m was selected for reasonably efficient pump absorption (~82%). The laser cavity was formed between the perpendicularly-cleaved fibre end-facet at the pump launch end of the fibre (which also served as the output coupler), and a simple external cavity comprising a collimating lens and a plane mirror with high reflectivity at ~1.8-2.1 μm at the other end of the fibre. A dichroic mirror with reflectivity >99.8% at ~2 μm and transmission >92 at ~1.5 μm was used to extract the output beam. The laser reached threshold at a launched pump power of 3.1W and produced a maximum output power of 19.2 W at 1991 nm at the maximum available pump power corresponding to 38.2 W launched. The slope efficiency with respect to the absorbed pump power was 69%, which compares favourably with the upper limit of ~78% determined by the Stoke efficiency. Wavelength tuning was achieved by modifying the external cavity design to include a simple diffraction grating (600 lines/mm) aligned in the Littrow configuration to provide wavelength selective feedback. In these experiments a shorter length of fibre (~2.5m) was employed and a simple arrangement for retro-reflecting the unabsorbed pump light after a single-pass to improve the pump absorption efficiency. Using this resonator configuration, we obtained a maximum output power of 17.4 W at 1941 nm for 38.2 W of launched pump power, and the lasing wavelength could be tuned over 200 nm from 1861 to 2061 nm with an output linewidth (FWHM) of <0.5 nm. For the core pumping experiments, similar cavity configurations were employed, but with a much shorter length of fibre (~24 cm) due to the higher absorption coefficient (~150 dB/m) for the pump light. For the non-tunable cavity configuration, a maximum output power of 12.1 W at 1861 nm was generated with a slope efficiency of 58.5% with respect to the absorbed pump power. For the tunable cavity, we obtained up to 8.4 W of output and operating wavelength was tunable over 248 nm from 1725-1973 nm at multi-watt power levels. The prospects for further improvement in performance will be discussed.

1. D. Y. Shen, J. I. Mackenzie, J. K. Sahu, W. A. Clarkson and S. D. Jackson, "High-Power and Ultra-Efficient Operation of a Tm³⁺-doped Silica Fiber Laser," *Advanced Solid-State Photonics* 2005, paper MC6, 2005.
2. Y. Jeong, P. Dupriez, J. K. Sahu, J. Nilsson, D. Shen, W. A. Clarkson, S. D. Jackson, "Thulium-ytterbium co-doped fiber laser with 75W of output power at 2 microns," *SPIE European Symposium on Optics and Photonics for Defence & Security* London 25-28 Oct 2004 Paper. 5620-4.

“The Contractor, University of Southampton” hereby declares that, to the best of its knowledge and belief, the technical data delivered herewith under Contract No. F61775-01-C0008 is complete, accurate, and complies with all requirements of the contract.

DATE: 29/01/06

Name and Title of Authorized Official:

Professor W. A. Clarkson

“I certify that there were no subject inventions to declare as defined in FAR 52.227-13, during the performance of this contract.”

DATE: 29/01/06

Name and Title of Authorized Official:

Professor W. A. Clarkson